energy&fuels

pubs.acs.org/EF

Article

Geochemical Impacts of CO_2 Mineralization in Carbonate and Basalt Formations: A Critical Review on Challenges and Future Outlook

Prince N. Y. M. Otabir, Aaditya Khanal,* and Fatick Nath

Cite This: *Energy Fuels* 2025, 39, 1226–1251

Read Online

ACCESS | Metrics & More | Article Recommendations

ABSTRACT: Carbon capture and storage (CCS) is an effective mitigation strategy to curb greenhouse gas emissions into the atmosphere. Although sandstone reservoirs have been widely used for CCS due to their favorable properties, their effectiveness is limited by slow mineral trapping. This review explores carbonate and basaltic formations as alternative CO_2 storage solutions. Basalt formations contain highly reactive minerals that promote rapid CO_2 mineralization. Pilot studies have demonstrated successful mineralization within 2 years. Carbonate formations also show promise for efficient CO_2 trapping. However, several challenges must be addressed. These include complex interactions between CO_2 and rock substrates, difficulties characterizing carbonate formations, and variable behavior in basalt formations under different conditions. This review comprehensively reviews and analyzes the current state of the art on the dissolution and mineralization processes in carbonate and basalt formations. Key issues such as reservoir characterization, changes in flow properties, and long-term CO_2 integrity are highlighted. Additionally, the review identifies critical challenges for large-scale storage, including costs, CO_2 injectivity, storage integrity, and effective monitoring techniques. Addressing these challenges is essential for realizing the potential of carbonate and basalt formations for efficient CO_2 storage. Successful implementation of these strategies will significantly contribute to mitigating climate change by providing a secure and permanent solution for greenhouse gas emissions.

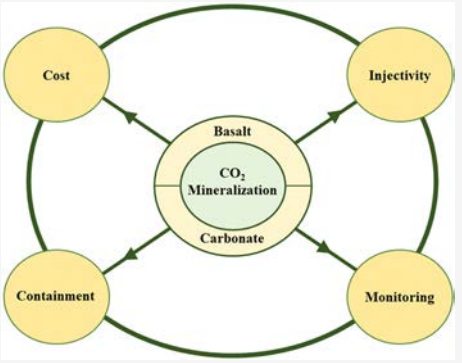

1. INTRODUCTION

The negative impacts of the increase in global surface temperature have become severe and frequent.[1] Research data from 1950 to 2022 shows that the global temperature has risen by 0.89 °C, which can be attributed to the increasing concentration of atmospheric greenhouse gases (GHGs), including nitrous oxide (N_2O), carbon dioxide (CO_2), methane (CH_4), and water vapor ($H_2O_{(g)}$). Global warming is caused by these gases primarily because they act as a thermal blanket that traps a significant amount of heat. Although $H_2O_{(g)}$ plays a substantial role in global warming, CO_2 concentration is the controlling factor due to its significantly long atmospheric residence time.[2] CO_2 is also abundant in the atmosphere due to daily human activities, including deforestation, the combustion of fossil fuels, industrial processes, and other various practices.[3,4] The impacts of climate change due to the increase in anthropogenic GHGs are quantifiable and well-documented. For instance, in 2023 alone, the U.S.A. experienced 25 confirmed "billion-dollar" weather and climate disaster events.[5] At a broader time scale, the inflation-adjusted cost of climate-change-related natural disasters amounted to over US$ 2.657 trillion, resulting in approximately 16,340 fatalities.[5] These disasters, such as droughts, floods, winter storms, and cyclones, have grown in severity and frequency worldwide, resulting in irreversible damage to both natural ecosystems and human societies.

With the global energy demand on the rise, there is a risk of further GHG emissions accumulating in the atmosphere, leading to increased global temperatures and potentially catastrophic consequences. In response, international initiatives have emerged to mitigate CO_2 emissions through policy reforms. At the 2015 United Nations Climate Change Conference in Paris, 195 different countries committed to reducing GHG emissions, aiming to limit global temperature increase to below 2 °C above preindustrial levels, with a target range of 1.5 to 2 °C.[6] More recently, at the 2023 UN Climate Change Conference (COP28), approximately 200 countries agreed to implement a quinquennial "global stocktake" to assess worldwide progress on climate action and support, identify the gaps, and collaboratively develop strategies to enhance climate action.[7] To limit the global temperature increase of 1.5 and 2 °C, the proposed solutions

Received: September 11, 2024
Revised: December 19, 2024
Accepted: December 20, 2024
Published: January 6, 2025

https://doi.org/10.1021/acs.energyfuels.4c04424
Energy Fuels 2025, 39, 1226–1251

include replacing the current fossil fuel-dominated energy supply chain with renewable energy sources and increasing fuel efficiency/conservation. One of the promising solutions expected to make a significant contribution to GHG abatement is carbon capture and sequestration (CCS), as illustrated in Figure 1.[8,9] CCS involves capturing CO_2 emissions from power plants and industrial settings, transporting them to storage sites, and permanently storing them.[10]

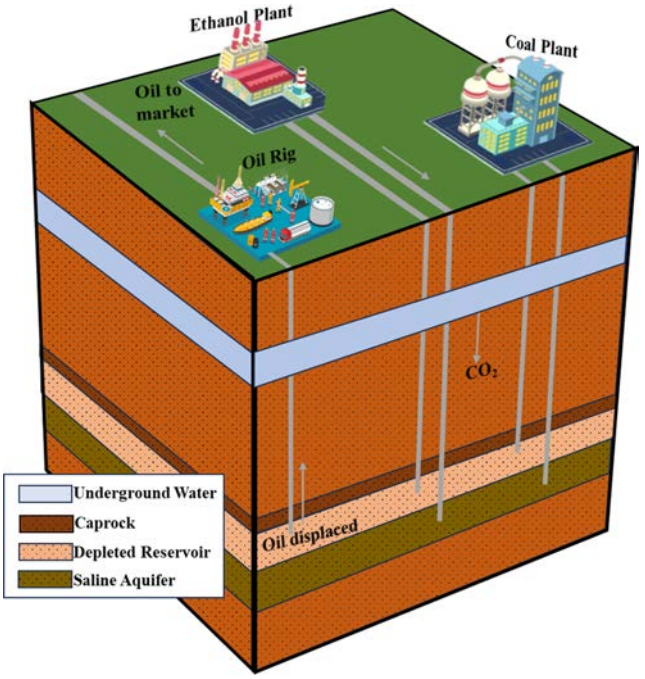

Figure 1. A schematic representation of CCS. CO_2 is captured from plant-emitting sources, such as ethanol and coal plants, and then injected into subsurface formations for storage. Reproduced with permission from ref 10. Copyright 2023 Congressional Budget Office.

The global status of CCS facilities has seen significant growth in recent years (see Table 1). As of 2024, the number of

Table 1. Current Global Status of CCS Facilities[11]

status of facility	number
operational	50
in construction	44
advanced development	248
early development	287
total	629

operational facilities has reached a total of 50, marking a 22% substantial increase from 2023. Moreover, the development pipeline has expanded rapidly, with a 60% surge over recent years, bringing the total number of facilities under development to 629.[11] This growth reflects a global commitment to advancing CCS technology to meet carbon reduction targets. The U.S.A. leads in CCS implementation, as evidenced by its high capture capacity (Figure 2) and the number of operational facilities (Table 2 shows the capture capacity of 18 operational facilities[10]).

Despite this progress, the existing and planned facilities are still insufficient to address the scale of CO_2 emissions from various industries, especially in the U.S.A., highlighting the need

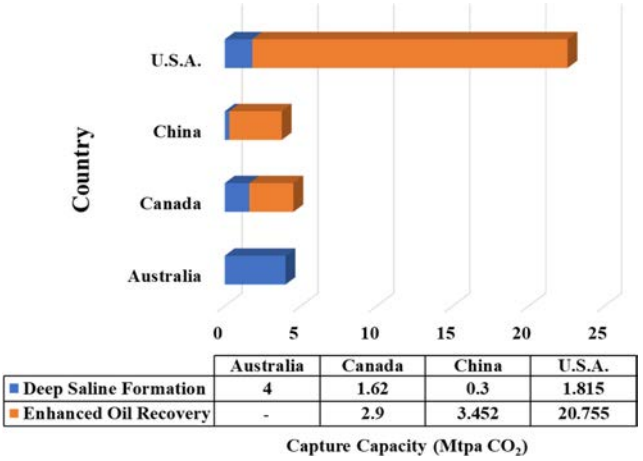

Figure 2. Capture capacity of CO_2 operational facilities in Australia, Canada, China, and the U.S.A. based on the storage codes.[11]

Table 2. CCS Facilities Operating in the U.S.A[10,11]

name of facility	location	year CCS begun	CO_2 capture capacity (MMT/year)	CO_2 storage formation
Terrell	Texas	1972	0.5	depleted oil/gas
Enid Fertilizer	Oklahoma	1982	0.2	sandstone
Shute Creek	Wyoming	1986	7.0	sandstone
Great Plants	North Dakota	2000	3.0	carbonate
Core Energy	Michigan	2003	0.35	shale
Arkalon	Kansas	2009	0.5	sandstone
Century Plant	Texas	2010	5.0	carbonate
Bonanza BioEnergy	Kansas	2012	0.1	sandstone/shale
Air Products	Texas	2013	0.9	sandstone
Coffeyville	Kansas	2013	0.9	fractured sandstone
Lost Cabin	Wyoming	2013	0.9	sandstone
PCS Nitrogen	Louisiana	2013	0.3	sandstone/carbonate
Petra Nova	Texas	2017	1.4	carbonate
Illinois Industrial	Illinois	2017	1.0	sandstone
Red Trail Energy	North Dakota	2022	0.18	sandstone
Harvestone Blue Flint	North Dakota	2023	0.2	sandstone
Barnett Zero	Texas	2023	0.185	carbonate
Bantam DAC	Oklahoma	2024	0.005	carbonate

for a comprehensive review of CCS to inform future research, development, and deployment efforts.

Three main types of geological formations are usually considered for the geo-sequestration of CO_2—coal beds, saline aquifers, and depleted oil and gas reservoirs.[12] Among the three types, saline aquifers possess the greatest storage capacity, primarily due to their location within highly porous and permeable sedimentary basins.[13] The global storage capacity for CO_2 in geological formations is estimated to be between 10,000 to 20,000 billion metric tons, with deep saline aquifers alone potentially accommodating up to 12 billion metric tons of CO_2.[14] In the U.S.A., deep saline aquifers have an estimated storage capacity of 8000−12,000 gigatons of CO_2.[15] These aquifers require fewer injection wells, facilitating easier pressure

https://doi.org/10.1021/acs.energyfuels.4c04424
Energy Fuels 2025, 39, 1226−1251

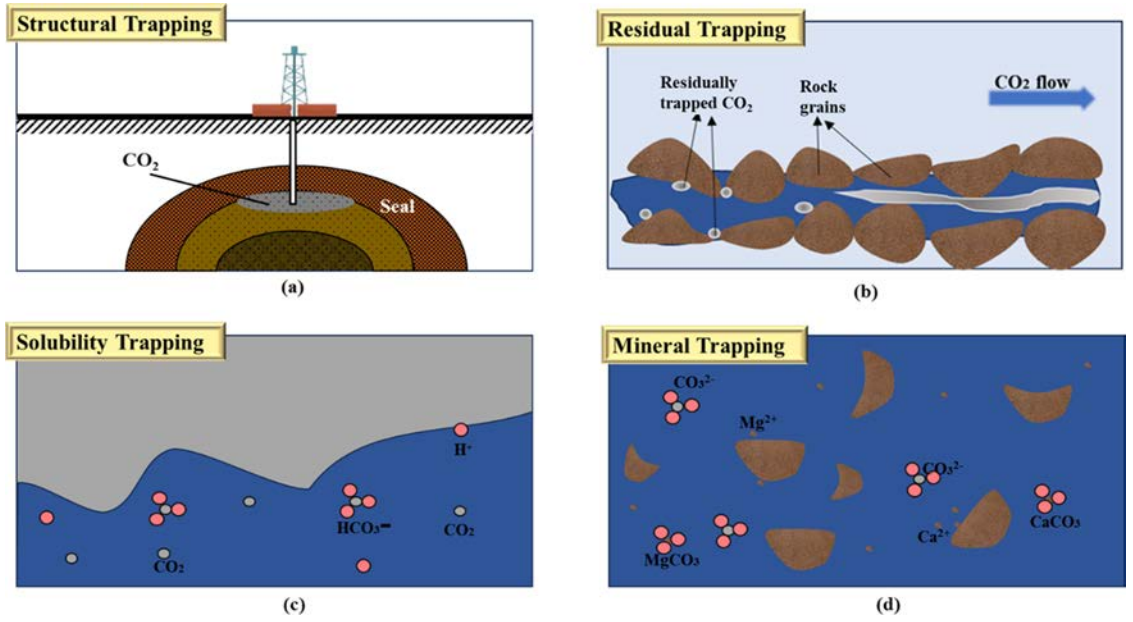

Figure 3. CO_2 trapping mechanisms in saline aquifers. Reproduced with permission from ref 22. Copyright 2022 Elsevier.

dissipation due to their highly porous and permeable characteristics.[16] Moreover, these aquifers are characterized by high salinity, which makes them unusable for basic human activities, further supporting their use in CO_2 sequestration.[13]

A suitable saline aquifer for CO_2 sequestration must have a low permeable rock layer, known as a caprock (or seal), above the aquifer.[17] This caprock is crucial for preventing the injected CO_2 from migrating into the atmosphere. As illustrated in Figure 1, the route to deep saline aquifers passes through underground freshwater sources, which could get contaminated due to a potential leakage through the caprock. Therefore, evaluating the integrity of caprocks is essential.[12] Zhang and Song[18] identified different mechanisms by which a caprock could fail—diffusive loss through the caprock, fault leakage, leakage through pore spaces when capillary breakthrough pressure has been exceeded, and leakage through injection wells when wells are degraded.

In saline aquifers, CO_2 can be stored as a supercritical fluid at a specific temperature (304.2 K) and pressure (7.376 MPa).[19] As a supercritical fluid, it exhibits the characteristics of both a liquid and a gas. Storing CO_2 in its supercritical state offers the advantage of reduced storage volume compared to gaseous CO_2.[20] During CO_2 injection into saline aquifers, the trapping mechanisms are vital in ensuring long-term storage over geologically significant time scales. Figure 3 illustrates the four main CO_2 trapping mechanisms: physical trapping (including structural and residual trapping) and geochemical trapping (including solubility and mineral trapping).[21]

Upon injection into the aquifers, CO_2 moves upward to the top of the reservoir and gets trapped by caprocks (Figure 3a).[17] This is known as the structural trapping mechanism, and it initially traps the maximum fraction of the injected CO_2 in the aquifer.[22] In response to the injection of CO_2, the saturation of water in the pores decreases while the CO_2 saturation increases, causing the CO_2 to be trapped in the pore and pore throat spaces between the rock grains (as shown in Figure 3b).[23,24] This process leads to the immobilization of CO_2, preventing it from migrating further and ensuring its long-term storage in the saline aquifer.[22] Figure 3c shows the solubility trapping mechanism, which occurs when a fraction of the injected CO_2 dissolves in the brine during migration.[25] Bachu[26] highlighted that depending on the brine's salinity, this migration of CO_2 occurs by diffusion of molecules, which takes place away from the boundary between the gas-aqueous two-phase zone, where there is dissolution into the underlying aqueous phase, ultimately raising the aqueous phase's density by 0.1−1%.[27] The denser phase sinks to the bottom of the aquifer, allowing the less dense CO_2-brine mixture to rise to the top.[28] This creates a loop ensuring the CO_2 is trapped as a dissolved phase, making solubility trapping the most important method for trapping CO_2.[29]

The solubility of CO_2 in brine not only plays a role in this trapping process but also serves as a precursor to mineral trapping. Mineral trapping involves geochemical reactions where stable, solid compounds like carbonates are formed when CO_2 interacts with the host formation's minerals (as shown in Figure 3d).[30] It is slower than the other trapping mechanisms; therefore, it may take hundreds to thousands of years, depending on the reservoir mineralogy, to see its full impact.[12,13] However, it is the only recognized permanent method of CO_2 storage, free from concerns related to CO_2 leakage.[31]

To effectively utilize mineral trapping, it is crucial to identify and characterize suitable storage reservoirs. This is particularly important for achieving climate goals, as vast volumes of CO_2 need to be stored. Carbonate and basalt formations are characterized by very reactive minerals, providing an attractive avenue for CO_2 sequestration through enhanced mineralization.[32] Studies demonstrate that the speed of mineralization of injected CO_2 can be significantly increased in basalt formations so that complete mineralization is observed in a minimum of 2−10 years.[33−35] However, the factors affecting the mineralization of CO_2 in these rock types are not yet fully understood. Over the past decade, numerous researchers have investigated and reviewed the reactions between these rock types and CO_2. For instance, Zevenhoven et al.[36] outlined the developments and trends since the IPCC special report on CCS[37] and discussed the developments toward large-scale application in basalts. Another review by Geerlings and Zevenhoven[38] discussed experimental studies on the interactions between basalts and CO_2. They

https://doi.org/10.1021/acs.energyfuels.4c04424
Energy Fuels 2025, 39, 1226−1251

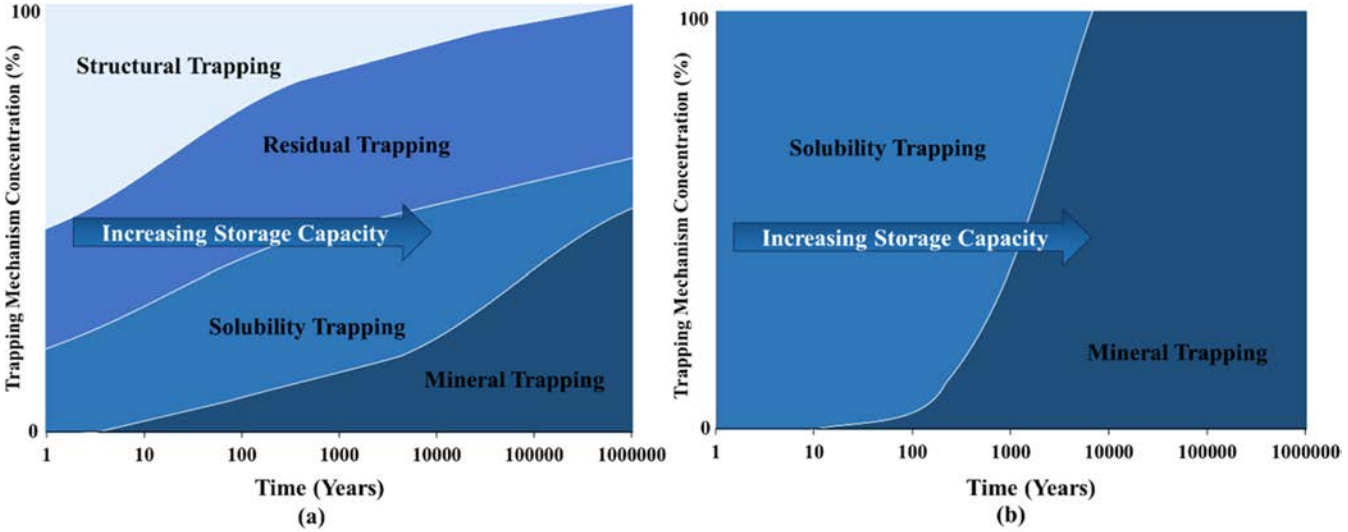

Figure 4. Comparison of CO_2 trapping mechanisms in (a) sedimentary basins and (b) basalts after injection of CO_2 into the reservoir. (a) is reproduced with permission from ref 56. Copyright 2022 International Energy Agency. (b) is reproduced with permission from ref 57. Copyright 2017 Elsevier.

highlighted heat-activated serpentine and magnesium silicates as methods for rapid carbon mineralization. Siqueira et al.[32] reviewed experimental and numerical studies employed for studying CO_2-water-rock interactions in carbonates. Bonto et al.[39] highlighted the challenges and enablers of large-scale CO_2 storage in carbonate formations. Some challenges were formation weakening, the integrity of the caprock, reactivation of faults in the formation, and injectivity. Raza et al.[40] presented a screening criterion for the selection of suitable basalt formations for the geological storage of CO_2. Eyinla et al.[41] reviewed the petrophysical alterations in carbonate formations during the injection of CO_2 for storage and Enhanced Oil Recovery (EOR) purposes. In the review of Kim et al.,[42] they focused on the carbon mineralization process in carbonates and basalts, highlighting temperature, rock type, fluid composition, competing reaction, nucleation, and injected CO_2 phase as the main factors affecting the mineralization process. Lu et al.[43] recently reviewed the experimental studies on basalt-CO_2 interactions, identifying research gaps and needs. Bashir et al.[44] also recently outlined the most recent advances in CCS technology. The recent advances in CCS technology include the integration of CO_2 storage with EOR and the commercialization of CCS projects.

Numerous reviews have primarily examined specific aspects of CO_2 mineralization in basalts or carbonates,[36,38,41,44] such as experimental studies or numerical modeling. A comprehensive review integrating both experimental and numerical studies and a detailed economic evaluation of large—scale CO_2 storage in these formation types is currently lacking. Given the recent advances in CCS technologies, particularly the commercialization of storage projects, a timely and critical review is needed to bridge these gaps and enhance understanding to ensure the effective deployment of CO_2 sequestration strategies. The objectives of this review, therefore, are to

- Clarify the key factors influencing dissolution and mineralization rates in basalts and carbonates.
- Enhance the understanding of how CO_2 mineralization affects reservoir flow properties.
- Conduct an economic evaluation of the potential costs associated with CO_2 storage in such rock types.
- Identify knowledge gaps and areas for future research.

By addressing these knowledge gaps and challenges, the findings of this review are not only timely, but essential for advancing CO_2 storage solutions.

2. CO_2 STORAGE IN BASALTIC FORMATIONS

Basaltic rocks present an ideal target for CO_2 storage due to their composition and structure. They are the most prevalent igneous rocks on Earth, with 45−53% SiO_2 content.[22] The mineral composition of basalts, contingent on magma composition and solidification conditions, may include olivine, pyroxenes, plagioclase feldspars, iron titanium (Fe−Ti) oxides, wollastonite, forsterite, serpentine/chrysotile, and anorthite.[45] These minerals, which are abundant in divalent cations such as Ca^{2+}, Mg^{2+}, and Fe^{2+}, give basalts superior mineralization capacity compared to other silicate-based rocks.[46]

The physical properties of basaltic rocks also contribute to their suitability for CO_2 storage. The porosity and permeability of basaltic rocks can vary significantly depending on their formation and subsequent alteration. Typical porosity values for basalts can range from 0.05−0.5[47] while permeability in basalts can span from 1.013×10^{-8}−1013 mD, with higher values often associated with fractured or vesicular basalts.[48]

Several basalt formations in the U.S.A., including Columbia River Basalt Group, Grande River Basalt Group, East Coast Basalt, Palisades, Hawaii olivine-rich basalt, Southeast Coastal plain basalts, offer promising sites for CCS through in situ mineral carbonation.[49−52] This process has gained attention as an effective carbon storage solution.

In-situ mineral carbonation involves the injection of captured CO_2 into underground reactive rocks for mineralization into stable carbonate minerals.[22] While this mineralization reaction occurs naturally through silicate weathering over geological time scales, artificial mineral storage can accelerate carbon fixation much faster.[53] By injecting CO_2 into the ground, solubility trapping occurs immediately, allowing for rapid carbon sequestration and bypassing the slow natural process of silicate weathering.[53] In a minimum of 2−10 years, a vast majority of the injected CO_2 is observed to be trapped as a carbonate mineral.[33−35,54] Mineral carbonation can be enhanced by

https://doi.org/10.1021/acs.energyfuels.4c04424
Energy Fuels 2025, 39, 1226−1251

Table 3. Mineral Dissolution Reactions of Basaltic Minerals upon Contact with CO_2[40,61,62]

mineral, chemical formula	reaction pathway
olivine (Forsterite), Mg_2SiO_4	$Mg_2SiO_4 + 2H_2CO_3 \rightarrow 2Mg^{2+} + H_4SiO_4$
serpentine, $Mg_3Si_2O_5(OH)_4$	$Mg_3Si_2O_5(OH)_4 + 3H_2CO_3 \rightarrow 3Mg^{2+} + 2H_4SiO_4 + H_2O$
anorthite, $CaAl_2Si_2O_8$	$CaAl_2Si_2O_8 + H_2CO_3 + H_2O \rightarrow Ca^{2+} + Al_2Si_2O_5(OH)_4$
wollastonite, $CaSiO_3$	$CaSiO_3 + H_2CO_3 + H_2O \rightarrow Ca^{2+} + H_4SiO_4$
pyroxene (Diopside), $CaMgSi_2O_6$	$CaMgSi_2O_6 + 2H_2CO_3 + 2H_2O \rightarrow Ca^{2+} + MgCO_3 + 2H_4SiO_4$

dissolving CO_2 in water prior to or during injection, enhancing solubility trapping, and achieving mineral trapping within 2 years at 20−50 °C.[55] This, thus, eliminates the risk of CO_2 migrating to the atmosphere due to the relatively fast dissolution rates and mineralization. As shown in Figure 4, mineralization occurs substantially faster in basalts than in sedimentary basins.

2.1. CO_2 Trapping Mechanism Process in Basaltic Formations. After injection into basaltic formations, CO_2 dissolves in water and gets trapped as an aqueous component[58] as expressed in eq 1. The aqueous CO_2 then reacts with H_2O to generate carbonic acid (eq 2).[59] Bicarbonate and hydrogen ions are produced when the carbonic acid dissociates further.[60]

$$CO_2(sc) + 3H_2O \rightleftharpoons CO_2(aq) + 3H_2O \quad (1)$$

$$H_2O + CO_2(aq) \rightleftharpoons H_2CO_3 \quad (2)$$

$$H_2CO_3 \rightleftharpoons HCO_3^- + H^+ \quad (3)$$

$$HCO_3^- \rightleftharpoons CO_3^{2-} + H^+ \quad (4)$$

The liberation of protons in this process causes the pH to decrease, a factor dependent on the temperature, CO_2 partial pressure, water salinity, and alkalinity.[46] A proton reaction occurs between basaltic glass and the primary basaltic minerals (i.e., pyroxene, olivine, plagioclase, etc.). This leads to the release of the divalent cations (Ca^{2+}, Mg^{2+}, and Fe^{2+}) for CO_2 mineralization expressed in eq 5.[33] Table 3 summarizes the dissolution reactions of some minerals that take place in basaltic formations.

$$\text{Basaltic glass} + H^+ \rightleftharpoons Ca^{2+} + Mg^{2+} + Fe^{2+} + \ldots \quad (5)$$

The dissolution of these basaltic minerals is the rate-limiting step in carbon mineralization, as it determines the divalent cations available for the mineralization of CO_2.[63] However, this process is complex and influenced by several factors, making it essential to understand these factors to optimize the sequestration of CO_2 in basalts. The key factors affecting basaltic mineral dissolution are:

2.1.1. Temperature. Temperature significantly influences the dissolution kinetics of basaltic rocks during the sequestration of CO_2. The Arrhenius equation below describes the relationship between dissolution reaction rate and temperature:

$$k = A \exp\left(\frac{-E_a}{RT}\right) \quad (6)$$

A is the pre-exponential factor, E_a is the activation energy, R is the gas constant, and T is the absolute temperature. As predicted by the Arrhenius equation, an increase in temperature results in a higher reaction rate. This is consistent with experimental studies such as those conducted by Gislason and Oelkers,[64] who observed an increase in dissolution rate as temperature increased from 6 to 50 °C. Similarly, Schaef and McGrail[65] reported a significant increase in dissolution rates of basalt samples from the Columbia River flood basalts, with rates increasing over 100 times as temperature rose from 25 to 90 °C. Rosenbauer et al.[66] investigated the impact of temperature on the reaction rate of tholeiitic basalts over a pressure of 300 bar and temperature range of 50−300 °C, and discovered the optimum extent and rate of reaction to be at 100 °C.

As shown in Figure 5, higher temperatures correspond to higher dissolution rates for diopside, forsterite, albite, crystalline basalts, and the other basaltic minerals further supporting the importance of temperature in basalt dissolution. However, Delerce et al.[67] recently extended this understanding by investigating altered basalts and found that while the release rates of divalent cations from altered basalts were one to 3 orders of magnitude slower compared to fresh crystalline basalt or basaltic glass, the temperature still played a crucial role. They observed a significant increase in release rates as the temperature rose from 100 to 120 °C, further highlighting the universal impact of temperature on basaltic minerals, whether altered or unaltered. These findings suggest that temperature plays a crucial role in the dissolution of basaltic minerals. Furthermore, understanding the effects of temperature on basalt dissolution can inform strategies for enhancing mineral carbonation reactions, such as injecting supercritical CO_2 into deeper formations, which may potentially speed up the dissolution of basalts.[68]

2.1.2. pH. The pH effect on basalt dissolution rates is complex and varies with each specific mineral. As presented in Figure 6, each mineral follows a unique path as pH increases from 3 to 10 at a constant temperature (25 °C). Oligoclase, andesine, glassy basalts, and crystalline basalts exhibit U-shaped variations with pH, with dissolution rates decreasing under acidic conditions but increasing under alkaline conditions. In acidic conditions, higher H^+ ion activity enhances the diffusion exchange between divalent cations and H^+ ions, resulting in increased ion release rates.[75] This aligns with the dissolution rate equations described below;[64,76]

$$r = k a_{H^+}^n \quad (7)$$

$$r_{+,geo} = k\left(\frac{a_{H^+}^3}{a_{Al^{3+}}}\right)^{1/3} \quad (8)$$

where k is the reaction rate constant, described in eq 6, a_i is the subscripted species activity, and n is the order of the reaction. As the activity of the H^+ ions increase, the dissolution rate increases.

The dissolution rates of oligoclase, crystalline basalts, glassy basalts, andesine, and diopside reach a minimum at neutral pH conditions, whereas the dissolution rate of crystalline basalts and glassy basalts continues to increase as the pH rises. This variation in dissolution patterns is attributed to the diverse mineral composition of these basalts.[70] As evident in Figure 6, acidic conditions generally promote the dissolution of all basaltic

https://doi.org/10.1021/acs.energyfuels.4c04424
Energy Fuels 2025, 39, 1226−1251

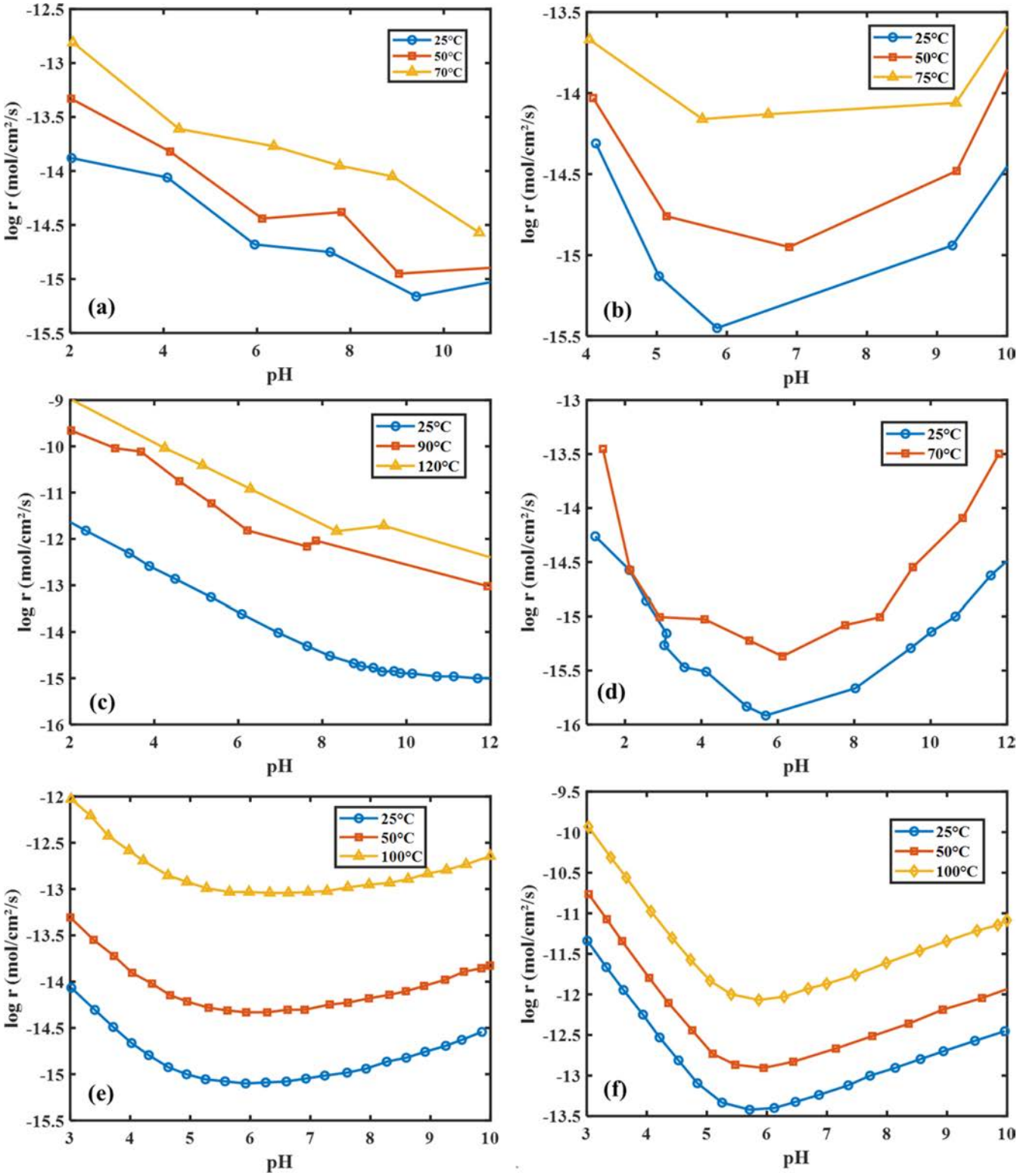

Figure 5. Effect of temperature on (a) diopside,[69] (b) crystalline basalts,[70] (c) forsterite,[71] (d) albite,[72] (e) andesine,[73] and (f) glassy basalts[74] at varying temperatures. Dissolution rates are more pronounced under higher temperatures for basaltic minerals.

minerals. In fact, the experimental work by Berger et al.[77] demonstrated that basaltic glass dissolution rates increase significantly under acidic conditions at high temperatures (150 °C), further supporting the notion that acidic conditions enhance dissolution rates.

2.1.3. Pressure. The pressure of the system may play a crucial role in controlling the dissolution rates of basaltic minerals. The injection of CO_2 into a system decreases the pH, which has a significant impact on basalt dissolution by increasing the concentration of dissolved H^+ ions. However, the effect of overall system pressure on the dissolution rate of basaltic

https://doi.org/10.1021/acs.energyfuels.4c04424
Energy Fuels 2025, 39, 1226−1251

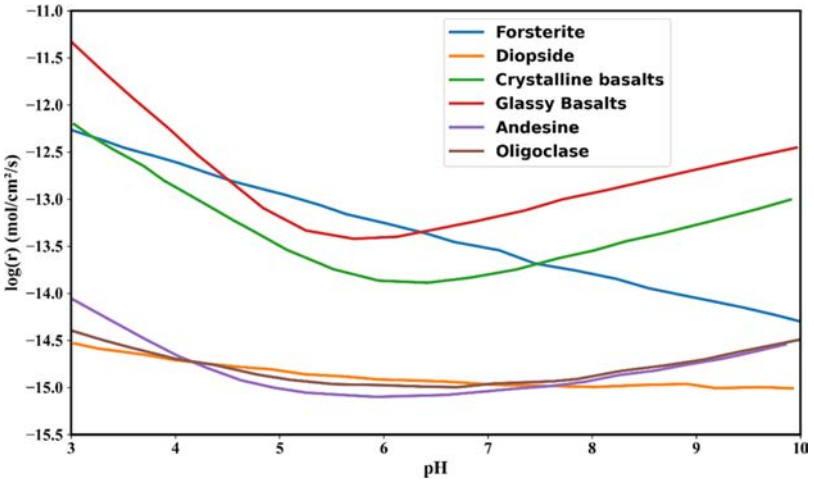

Figure 6. Dissolution rates of forsterite,[71] diopside,[69] oligoclase,[73] andesine,[73] and crystalline and glassy basalts[74] over pH range 3−10 at 25 °C. These dissolution rates represent the release rates of silicate ions from the basalt minerals, which is an essential process in mineral carbonation. The rates are expressed in units of mol/cm^2/s, indicating the amount of silicate ions released per unit surface area of the mineral per second.

minerals remains unclear. Dou et al.[78] investigated the influence of higher pressures and temperatures on basalt dissolution and observed that pressure had a negligible effect on reaction rates compared to the more substantial influence of temperature. This highlights that system pressure, while important, may not be the dominant factor in controlling dissolution rates, suggesting that more research is needed to clarify its role.

At the same time, the partial pressure of CO_2 also plays a crucial role in controlling the dissolution rates of basaltic minerals. Research has consistently shown that increasing the CO_2 partial pressure leads to a further decrease in pH, which in turn increases the dissolution rates of silicate minerals. For example, Wang and Giammar[79] observed a pH reduction of 0.5 when the CO_2 partial pressure was increased from 10 to 100 bar after injecting CO_2 at 25 °C, and a 6.5 faster dissolution rate of forsterite. In the experimental study of Prigiobbe et al.,[80] they observed similar results. They reported a reduction in pH upon increasing the CO_2 partial pressure from 0.2−10 MPa, which enhanced the dissolution of olivine. These findings demonstrate while CO_2 partial pressure significantly affects the dissolution of basaltic minerals, the role of overall system pressure in combination with the partial pressure of CO_2 remains underexplored. This gap in knowledge suggests that both pressure parameters should be considered in future studies to comprehensively understand their combined effects on mineral reactivity.

2.1.4. Other Influencing Factors. Several additional factors affect basaltic mineral dissolution. Salinity, for instance, has been found to have conflicting effects on dissolution rates. Wang and Giammar[79] reported that increased salinity (NaCl) increases the dissolution rates of basaltic minerals, while Stillings and Brantley[81] observed a reduction in the dissolution rate of feldspar after increasing the concentration of NaCl.

The presence of impurities in the CO_2 stream can also impact the dissolution rates. These impurities include hydrogen sulfide (H_2S), sulfur dioxide (SO_2), nitrogen oxides (NO_x), and others, which are often present in small percentages in captured CO_2. The addition of H_2S, for example, increases the dissolution rate of the basaltic minerals[82] due to the increased reactivity between basalt and CO_2.[65] Similarly, Flaathen et al.[83] found that adding aqueous sulfate to injected CO_2 increases the dissolution rate of basaltic minerals. Min et al.[84] observed an enhanced dissolution rate of anorthite when sulfate was added to the CO_2 stream. Additionally, the presence of nonreactive phases in heterogeneous rock materials increases the complexity of the prediction of the dissolution of minerals in basaltic formations.[85] In the experimental work of van Noort et al.,[85] they report that the presence of less reactive minerals did not slow down the dissolution rate of peridotite. In contrast, Wang et al.[86] recently investigated the dissolution characteristics of naturally altered basalts and compared them to unaltered basalts in CO_2-rich brine. Their results indicated that the release rates of divalent cations in altered basalts were an order of magnitude lower than those observed in unaltered basalts.

Organic ligands, including citrate, acetate, and oxalate, accelerate basalt dissolution by facilitating metal cation exchange and adsorption through surface complexation.[87] This process promotes the formation of reactive surface sites, thereby increasing the reactivity of basaltic minerals and accelerating dissolution rates.[88] Guy and Schott[89] noted that the diffusional transport of metals from basaltic glass surfaces significantly influenced dissolution rates. Similarly, Wolff-Boenisch et al.[90] observed that the presence of organic ligands enhanced the dissolution rates of basaltic glass; however, no significant ligand-promoting effect was noted in peridotite. Additionally, fluoride has been shown to promote the dissolution of basalt minerals through its complexation effect.[91] Under acidic conditions, the dissolution rates of the minerals increase with an increasing concentration of fluoride. The interactions between organic ligands and basalts remain complex, requiring further research.

Salinity, impurities in the CO_2 stream, nonreactive phases in heterogeneous rock materials, and organic ligands significantly impact dissolution rates. Understanding the effects of these factors is crucial to accurately predicting the behavior of dissolution rates in basaltic formations, and further research is needed to uncover the underlying mechanisms controlling basalt dissolution rates.

2.2. Carbonate Precipitation in Basalts and Effect on Flow Properties. Carbonate mineral precipitation, which involves the reaction of dissolved minerals with CO_2 to form carbonate minerals, is a crucial step in the carbon sequestration process, as it permanently stores CO_2 in solid mineral form (see Figure 7). Basaltic mineral dissolution facilitates this process by

https://doi.org/10.1021/acs.energyfuels.4c04424
Energy Fuels 2025, 39, 1226−1251

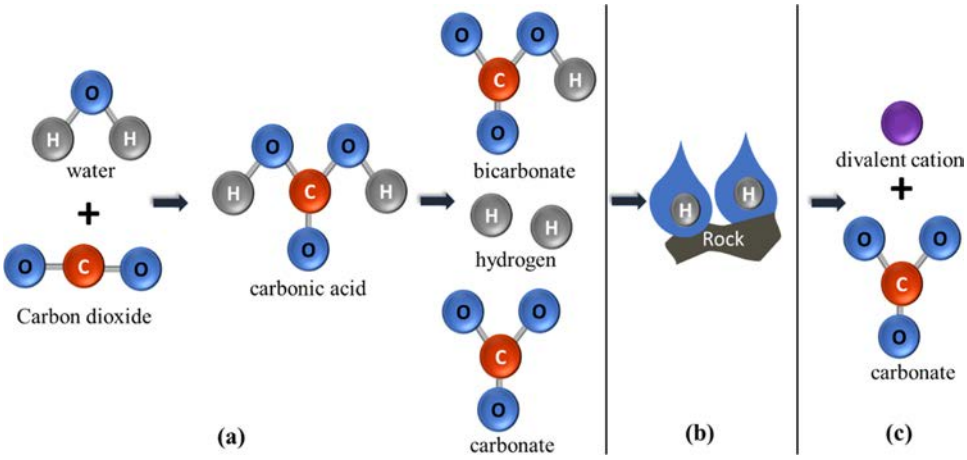

Figure 7. Process of carbon mineralization upon CO_2 injection into basalt formations, showing (a) CO_2 dissolution into formation water, (b) basaltic mineral dissolution driven by the resulting acidic environment, and (c) precipitation of carbonate minerals from cations released during mineral dissolution. Reproduced with permission from ref 42. Copyright 2023 Elsevier.

Table 4. Chemical Precipitation Reactions in Basalts[92,93]

mineral	chemical reaction
calcite	$Ca^{2+} + CO_2 + H_2O \leftrightharpoons \underbrace{CaCO_3}_{\text{Calcite}} + 2H^+$
magnesite	$Mg^{2+} + CO_2 + H_2O \leftrightharpoons \underbrace{MgCO_3}_{\text{Magnesite}} + 2H^+$
dawsonite	$Na^{2+}Al^{3+} + CO_2 + H_2O \leftrightharpoons \underbrace{NaAl(CO_3)(OH)_2}_{\text{Dawsonite}}$
siderite	$Fe^{2+} + CO_2 + H_2O \leftrightharpoons \underbrace{FeCO_3}_{\text{Siderite}} + 2H^+$
ankerite	$Fe^{2+} + Mg^{2+} + Ca^{2+} + CO_2 + H_2O \leftrightharpoons \underbrace{Ca(Fe, Mg)(CO_3)_2}_{\text{Ankerite}} + 2H^+$

consuming H^+ ions and increasing pH, promoting carbonate precipitation.[68] Table 4 summarizes some of the chemical precipitation reactions of potential carbonates that are formed in basaltic formations.[63] Despite similar mineral compositions, predicting specific carbonate precipitates remains challenging due to complex CO_2-basalt interactions.

Moreover, these dissolution–precipitation reactions significantly alter the pore network of basalts, impacting their flow properties. Rock dissolution can increase permeability and porosity, while mineral precipitation in pores and pore throats can decrease them. The dominant process determines whether the pore network becomes more connected or disconnected, affecting the overall flow properties.[94] Understanding these interactions is crucial, and numerous numerical and experimental studies have been conducted to investigate the complex dynamics between CO_2 and basaltic rocks (see Table 5).

The types of carbonates that precipitate in basalts are influenced by pressure and temperature conditions. At higher temperatures, the dissolution rate of basaltic minerals increases, resulting in a higher concentration of divalent cations, which can readily lead to the precipitation of carbonate minerals. Rosenbauer et al.[66] carried out carbon mineralization experiments for 4300 h on basaltic rocks composed of plagioclase, pyroxene, and olivine and observed that the precipitation of iron-bearing magnesite occurred mostly at 100 °C and at higher partial pressures of CO_2. Similarly, Xiong et al.[95] reacted basalt samples composed of plagioclase, pyroxene, and basaltic glass with pure water at a temperature and pressure of 100 °C and 10 MPa, respectively. The basalt cores were removed after 6, 20, and 40 weeks, and they observed the precipitation of carbonates. Voigt et al.[96] conducted batch experiments on basalt powder at 130 °C and noted the precipitation of smectite and aragonite at 0.25 MPa. However, at 1.6 MPa, there was magnesite precipitation as carbonates, which was three times higher than the initial carbonates mineralized at lower CO_2 partial pressure. These highlights the importance of high temperature and pressure conditions for the precipitation of carbonates in basalts.

Carbonate precipitation in basalts is also affected by the composition of the injected fluid and the formation water. Several studies have highlighted the advantages of using seawater as an injection fluid, particularly in terms of reaction rate and economic efficiency.[42] Wolff-Boenisch[97] noted that the pH buffering capacity of the reaction between CO_2-rock-fluid in basalts can be enhanced in alkaline groundwater or seawater. Building on this, Wolff-Boenisch and Galeczka[98] used synthetic seawater with a pH of 8.1 as an injection fluid to investigate the reactivity of crystalline and glassy basalts postinjection, observing continuous carbon mineralization in the form of Ca and Mg carbonates. Similarly, Voigt et al.[96] used North Atlantic seawater in a carbon mineralization experiment and observed a high reaction rate in the precipitation of carbonates. Rigopoulos et al.[99] conducted reactions between artificial seawater and either peridotite or very fine-grained basalt at room temperature for a duration of 2 months, identifying the mineralization of CO_2 in the form of aragonite ($CaCO_3$). Luhmann et al.[100] performed flooding experiments on basalt cores using brine solutions

https://doi.org/10.1021/acs.energyfuels.4c04424
Energy Fuels 2025, 39, 1226−1251

Table 5. Recent Studies on CO_2-Basalt Interactions under Different Conditions

reference	rock constituents	method	aqueous matrix	pressure (MPa)	temperature (°C)	duration	carbon precipitates
			experimental studies				
102	ankerite, quartz, chlorite, calcite	triaxial experimental test	water	150	25, 250	2 days	chlorite or smectite group
113	forsterite	batch reactor	deionized water	0.1,10	30−95	692 h	magnesite
105	olivine	autoclave	brine	13.5	185	n/a	magnesite
65	plagioclase, pyroxene,	batch reactor	water	10	60	180 days	calcite, pyrite, and marcasite
103	peridotite	flow through	1 mol/L NaCl + 0.6 mol/L $NaHCO_3$	11	160	200−450 min	siderite and magnetite
112	basaltic glass	batch reactor	water	0.2−1.3	40	260 days	ankerite, ferrihydrite, and smectite
66	plagioclase, pyroxene, olivine	batch reactor	NaCl	30	50−200	4300 h	Fe-bearing magnesite
107	peridotite	batch reactor	water	20	100−200	6 weeks	ferroan magnesite
106	olivine	flow through	artificial seawater	28	150	55.8−92.4 h	serpentine and hematite
109	plagioclase, pyroxene, amygdule, olivine	fabricated triaxial chamber	water	0.25	n/a	30−90 days	calcite
100	crystalline basalts	autoclave	NaCl	15	150	0.51−32.81 days	siderite
99	peridotite	batch reactor	seawater	0.101	25	2 months	aragonite
95	plagioclase, pyroxene, basaltic glass	batch reactor	water	10	100	6−40 weeks	aragonite and calcite
111	stapafell basaltic glass	batch reactor	water	8	50	12 h	siderite
104	livine	flow through	brine	20−25	185	92.88−333.34 h	magnesite
110	basaltic glass	batch reactor	Na_2CO_3	n/a	80−150	21−52 days	Ca-carbonates, smectite
101	augite, anorthite	batch reactor	water	0.43	20	65 days	calcite, aragonite
108	andesine, augite, olivine	flow through	seawater	2	21	1−3.5 months	n/a
			numerical simulation studies				
117	fractured basalts	numerical simulation	n/a	10	100	6 weeks	calcite, magnesite, siderite, manganese
114	basalt	numerical simulation	brine	7.5	33	10 years	calcite, magnesite, siderite, montmorillonite
115	basalt	numerical simulation	water	12.8	220	10 years	ankerite
116	basalt	numerical simulation	0.1 g/mol NaCl	13.5	50.5	200 years	magnesite and calcite
118	basalt	numerical simulation	3 g/mol NaCl	20.3	89.6	-	albite and magnetite

composed of CO_2-rich NaCl and suspected formation of siderite based on the calculated liquid saturation states. Schaef et al.[65] reported that the addition of H_2S leads to the precipitation of iron sulfides, which has the tendency to slow down the formation of carbonates in one basalt sample (Newark Basin Basalt) while increasing reactivity in another (Karoo basalt). These findings suggest that the reactivity of carbon mineralization is highly dependent on the composition of both the injection fluid and the formation water.

Pajdak et al.[101] conducted an experimental study on basalt samples from the Central European Volcanic Province in Poland using a geochemical reactor, where they observed an increase in porosity and pore volume due to the dissolution of rock minerals. This dissolution-driven porosity increase suggests that basalts have potential for CO_2 storage applications, as mineral dissolution can enhance the permeability of the formation. However, the precipitation of secondary minerals, such as carbonates and clays, can counteract this effect by reducing permeability and other flow properties. Several studies have reported permeability reductions in basalts due to mineral precipitation. In the experimental study of Kato et al.,[102] they reported a reduction in the permeability of basalts from an ancient fault zone, attributed to clay minerals precipitation. Similar results were reported by Andreani et al.[103] They noted a permeability reduction when low flow rates were employed. Also, the carbonate precipitation only decreased porosity in zones where diffusion-controlled transport was dominant. Peuble et al.[104] observed decreased permeability in olivine samples upon magnesite precipitation at 185 °C and 20−25 MPa. Béarat et al.[105] noted similar magnesite precipitation in the presence of brine and CO_2 on olivine at similar temperature conditions but at lower pressure (13.5 MPa). Godard et al.[106] conducted a core flooding experiment using olivine at a slow injection rate of 0.2 mL/h, finding that the olivine became impermeable after just 23 days despite a relatively small decrease in porosity of less than 4%. Hövelmann et al.[107] noted decreased porosity linearly correlated with the degree of olivine carbonation in high-temperature, high-pressure experiments. Building on these earlier studies, Stavropoulou et al.[108] conducted one of the most recent and comprehensive investigations on basalt's flow properties after exposure to dissolved CO_2 in seawater. Using X-ray computed tomography (XRCT), they mapped the 3D pore network of basalt cores and observed reductions in permeability and porosity, especially in micropores (<50 μm), due to CO_2 mineralization. Guha Roy et al.[109] conducted experiments to determine the stability of basalts for CCS. They noted strength loss in different basalt samples reacted with CO_2 and water at 0.25 MPa for 30−90 days. Their results showed that the samples with the highest reactivity showed the greatest strength deterioration, with the extent of

https://doi.org/10.1021/acs.energyfuels.4c04424
Energy Fuels 2025, 39, 1226−1251

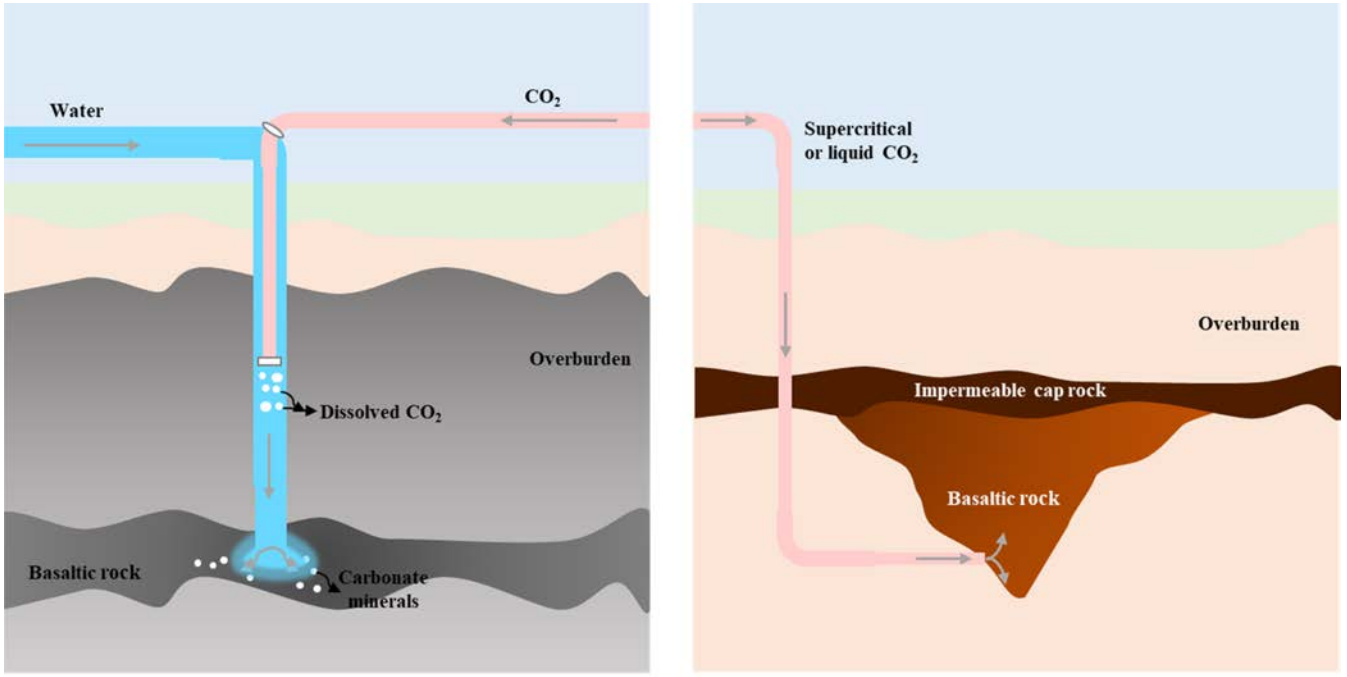

Figure 8. Carbon injection methods in basalt rocks. (a) Carbonated water injection, where CO_2 is dissolved in water before injection, and (b) Direct CO_2 injection, where pressurized liquid CO_2 is injected directly into the formation. The carbonated water injection method was used in the CarbFix pilot project, while the direct CO_2 injection method was used in the Wallula pilot project. Reproduced with permission from ref 123. Copyright 2014 American Association for the Advancement of Science.

strength loss depending on exposure time, mineralogy, and rock texture.

There are several other factors affecting the precipitation of carbonates in basalts which are not yet fully understood. In the experimental study of Hellevang et al.,[110] they found no carbonate formation at pH < 8 (80 °C) and pH < 7 (100−150 °C), but observed Ca-carbonates and smectite at higher pH. In contrast, Clark et al.[111] conducted water-basalt glass reactions that resulted in high pH (9−10), where no mineral precipitation was observed; however, siderite was identified as a thermodynamically stable mineral. Gysi and Stefansson[112] performed batch experiments on basaltic glass to study the feasibility of low-temperature (40 °C) CO_2 storage in basalts and noted mineralization of CO_2 into smectites and other carbonates. Additionally, Giammar et al.[113] investigated the conditions favorable for forsterite dissolution in water in the presence of supercritical CO_2 and reported the precipitation of magnesite. They employed magnesite seeds and observed faster magnesite precipitation in its presence. These studies suggest that the pH and specific mineral compositions significantly influence carbonate precipitation in basalts. While higher pH and the presence of certain minerals, like magnesite seeds, appear to promote carbonate formation, the exact mechanisms and conditions that favor different types of carbonate precipitation in basalts require further investigation.

Numerical simulation software are being employed to understand the reactions between basalts and CO_2 in subsurface formations. Wu et al.[114] conducted simulations using Transport Of Unsaturated Groundwater and Heat Reactions (TOUGH-REACT) on fractured basalts to investigate CO_2 mineral trapping and permeability changes. Their findings indicated that the mineralization of CO_2 leads to a reduction in porosity, which causes a permeability reduction. Additionally, they observed free-phase CO_2 accumulation at intersections of fracture, diverging into branching fractures. The predominant mineral formed during this process was calcite, with siderite and magnesite being formed in appreciable amounts. Erol et al.[115] reported limited mineral carbonation of ankerite due to pH and CO_2 mass fraction constraints in the Kizildere reservoir using TOUGH-REACT. In the numerical simulation study of Al Maqbali et al.,[116] they employed the Computer Modeling Group (CMG) simulation tool, and their results indicated 97% mineralization of injected CO_2 into calcite and magnesite, which led to a 5% reduction of the porosity. Menefee et al.[117] developed computer models with CrunchTope to study how CO_2 reacts with rocks in underground formations. They found that the overall mineral composition of the rocks does not significantly affect the amount of CO_2 that is stored, but it does influence how quickly and extensively the CO_2 is trapped in the rocks. This process tends to occur in areas where fluids flow slowly or in dead-end fractures. Zhao et al.[118] numerically investigated the interactions between altered and unaltered basalt, CO_2, and formation water in the Jianghan Basin, Central China, using TOUGH-REACT. They found reduced CO_2 mineral trapping for unaltered basalt compared to altered basalts, which aligns with the experimental results from Delerce et al.[67] that indicated slower cation release rates in altered basalts. These studies highlight the vital role numerical simulation software plays in predicting and understanding the complex interactions between CO_2 and basalt formations.

Recently, machine learning algorithms have been employed to enhance the prediction and monitoring of petrophysical properties and CO_2 storage.[119] Tariq et al.[120] developed a neural network model to predict the wettability behavior of Saudi Arabian basaltic rocks in CO_2-brine systems with high accuracy (0.93 training, 0.95 testing). Song et al.[121] used

https://doi.org/10.1021/acs.energyfuels.4c04424
Energy Fuels 2025, 39, 1226−1251

artificial neural networks to predict CO_2 storage efficiency in relation to basalt physical properties with 0.98 accuracy. These advancements in machine learning complement numerical simulations by providing high-accuracy predictions and monitoring capabilities, further advancing our understanding of CO_2 storage and behavior in basalt formations.

Despite these advancements in experimental, numerical, and machine learning approaches, the underlying mechanisms and kinetics of CO_2 storage in basalt rocks remain incompletely understood. Further research is necessary to optimize basalt's potential for carbon sequestration.

2.3. Field Mineral-Carbonation Studies in Basalts. For more than two decades, CO_2 mineralization in basaltic formations has been acknowledged as a viable carbon storage method. Currently, only two projects worldwide actively inject CO_2 into basalts: the CarbFix project in Iceland and the Wallula project in the U.S.A.[40] The details of the pilot projects (Wallula and CarbFix projects) are discussed below.

2.3.1. CarbFix Project. The CarbFix project, initiated in 2012 near Iceland's Hellisheidi geothermal power station, aimed to inject 30,000−40,000 tons of CO_2 annually into a basalt formation.[92] The target formation, at 400−800 m depth, exhibits vertical and lateral intrinsic permeabilities of 1700 and 300 mD, respectively.[53] The formation is composed of olivine tholeiite, a type of basaltic lava and hyaloclastite, with temperatures ranging from 20 to 50 °C and pH between 8.4 and 9.4.[92,122] Only pure CO_2 and CO_2+H_2S mixtures dissolved in water were considered for injection into the basaltic rocks (see Figure 8a).

The project used reactive and nonreactive tracers along with isotopes to calculate the mineral carbonation process. After 2 years of injections, the calculations indicated 95% CO_2 mineralization.[55,57] However, the injection increased subsurface biota, which contributed negligibly to the mineral carbonation process.[124]

Following initial success, the project expanded in 2014 to depths exceeding 1300 m and temperatures above 250 °C, allowing for the sequestration of a more significant percentage of CO_2.[82,125] Since 2014, the injection rate has increased annually, with estimates suggesting 60% mineralization achieved within 3 years.[115] Currently, the CarbFix project captures and stores approximately 33% of CO_2 and 68% of H_2S emissions from the Hellisheidi geothermal power station.[126]

2.3.2. Wallula Project. In 2013, the Wallula Project in Washington's Columbia River Basalt in Wallula, USA, began after a four-year initiation phase. Approximately 1000 tons of pure, liquified CO_2 were injected into the target formation, situated at depths between 828 and 887 m.[127] The formation consists of quartz tholeiites, dominated by augite, plagioclase, and glassy, noncrystalline mesostasis material.[128] The average temperature is 36 °C, with a flowtop characterized by porosity and permeability of 0.15−0.25 and 75−150 mD, respectively.[127] However, the layer between basalt flows (interflow) has very low permeability.

Prior to injection, the CO_2 was stored in tanks, pressurized, and heated. It was then injected into two fractured basalts (brecciated zones), and the reactions between the CO_2, basalt rocks, and formation water in the subsurface were closely monitored (see Figure 8b).[129] A perfluorocarbon tracer was used for a fluid temperature survey.[130] The survey showed that some of the injected CO_2 remained trapped as free-phase CO_2 within the interflow zone. Sidewall cores showed spherical carbonate nodules made of ankerite, confirming that a percentage of the injected CO_2 had undergone mineralization within 2 years of injection. Calculations indicate that over this period, approximately 60% of the total injected CO_2 was mineralized.[131]

Building on the success of these projects, there has been a growing interest in exploring basaltic formations for CCS worldwide. Tencent launched the CarbonX project in 2023 to advance the development of CCS technology in China. The project aims to develop and deploy CCS technology for storing CO_2 in basaltic formations in Guangdong Province, China, due to its suitable geological conditions.[132] Concurrently, the international PEBRAS project (Permanent sequestration of gigatons of CO_2 in continental margin basalt deposits) unites ten business companies and research institutions from Germany, Norway, the U.S.A., and India. This collaborative effort focuses on investigating the potential for storing CO_2 in marine basalt structures, which could offer significant storage capacity.[133] These initiatives highlight a global trend toward leveraging basaltic formations for CCS.

3. CO_2 STORAGE IN CARBONATE AQUIFER FORMATIONS

Carbonate formations are being recognized as an attractive CO_2 storage option since a significant portion of the world's oil reserves (approximately 60%) are found within these formations. When combined with enhanced oil recovery (EOR) techniques, carbonate formations become even more attractive storage targets.[134] Moreover, it can be assumed that since carbonate reservoirs could trap hydrocarbons for millions of years, they would effectively trap injected CO_2 for millions of years through a combination of the chemical and physical CO_2 trapping mechanisms.[135] However, the suitability of a particular carbonate formation for CO_2 storage ultimately depends on its specific mineral composition and chemical reactivity with the injected CO_2.

The predominant minerals found in carbonate rocks include dolomite and calcite.[136] However, they can also contain various other minerals, including glauconite, phosphate, and clay minerals. Additionally, secondary minerals like anhydrite, chert, quartz, ankerite, pyrite, and siderite can be present.[137] These minerals are highly susceptible to dissolution, especially by carbonic acid (H_2CO_3).[136,138] As such, the interaction between the fluids and rocks within carbonate formations is expected to be complex. In addition, carbonate rocks exhibit significant heterogeneity with regard to their permeability and porosity distributions−tight, vuggy, and fractured carbonates are the common types.[139] Typical porosity values range from 0.05−0.5, with the most productive reservoirs exhibiting porosities between 0.05−0.3.[140] Permeability in carbonate rocks is highly variable, spanning from less than 0.1 mD to over 1000 mD. This heterogeneity is further reflected in the various types of carbonate rocks, including dolostone and limestone, which have distinct mineralogical compositions. Dolostone, for example, typically consists of significant percentages of dolomite or calcium magnesium carbonate ($CaMg(CO_3)_2$), (>50 wt %). Calcite and anhydrite are also present in dolostones but in lower concentrations.[141] Limestone, conversely, has a high calcium concentration in the form of calcite ($CaCO_3$) and a much lower magnesium (Mg) concentration in the form of magnesium carbonate ($MgCO_3$).[142]

When CO_2 comes into contact with formation water (or brine) in carbonate rocks, dissolution into formation water (or

https://doi.org/10.1021/acs.energyfuels.4c04424
Energy Fuels 2025, 39, 1226−1251

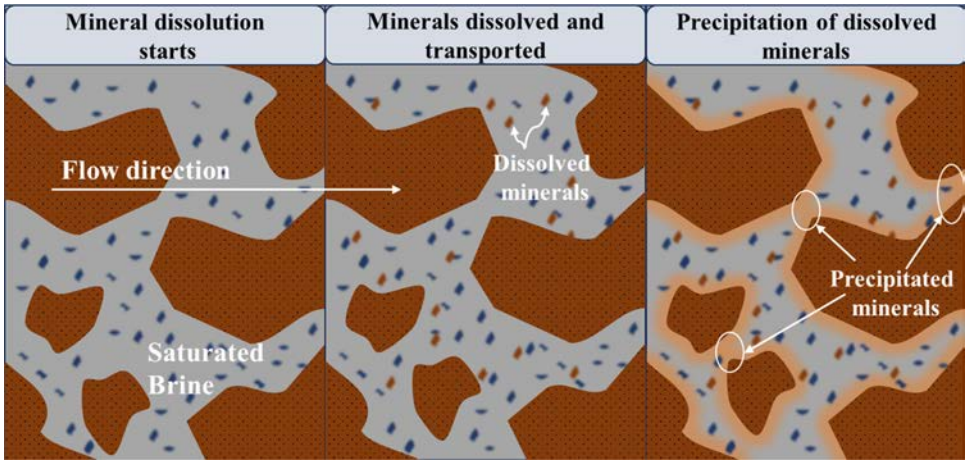

Figure 9. Schematic depicting the processes of mineral dissolution and precipitation in carbonate reservoirs, highlighting how CO_2 interaction leads to reduced permeability through the dissolution, transportation, and precipitation of minerals. Reproduced with permission from ref 141. Copyright 2017 Elsevier.

brine) takes place, where a slightly acidic solution is produced.[138] Reactions 1−4 depict the CO_2 dissolution reactions that take place in carbonate formations. CO_2 dissolution in the brine leads to a decrease in the pH of the brine, which facilitates the dissolution of the carbonate minerals in the reservoir, leading to an increase in the concentrations of divalent ions in the brine.[143] This leads to a complex series of chemical reactions that have the potential to alter the petrophysical properties of the rock (see Figure 9).[141] To date, only a few studies have focused on the dissolution of the minerals in carbonate aquifer formations, which will be discussed in the following sections.

3.1. Reaction with Limestone. The reactions between CO_2, formation brine, and calcite in limestone reservoirs can be expressed as follows:[136]

$$CaCO_3 + CO_2 + H_2O \leftrightarrow Ca^{2+} + 2HCO_3^- \quad (9)$$

$$CaCO_3 + H^+ \leftrightarrow Ca^{2+} + HCO_3^- \quad (10)$$

$$CaCO_3 + H_2CO_3 \leftrightarrow Ca^{2+} + 2HCO_3 \quad (11)$$

These reactions are paramount in carbon sequestration in carbonate reservoirs, as they alter the arrangement of the pores in the rocks.[144] Specifically, the dissolution of calcite is accelerated by the presence of CO_2-releasing H^+ at the calcite surface.[145] This process leads to a reduction in the pH of the reservoir brine, causing the dissolution of calcite and an increase in alkalinity (HCO_3^-).[146] Furthermore, this process involves not only the dissolution of the minerals but also the transport and subsequent precipitation of minerals within the pore spaces of the rock. These reactions are primarily influenced by three factors: the CO_2 partial pressure, the temperature of the reservoir, and the acidity (pH) of the pore fluids.

3.2. Reaction with Dolostone. In dolostone reservoirs, the interactions between dolomite, formation brine, and CO_2 are as well important, as they trigger a series of reactions that could greatly impact the petrophysical properties of the rocks. The reactions involved can be described as follows:[138]

$$2H^+ + CaMg(CO_3)_2 \leftrightarrow Mg^{2+} + Ca^{2+} + 2HCO_3^- \quad (12)$$

$$CaMg(CO_3)_2 + 2H_2CO_3 \leftrightarrow Mg^{2+} + Ca^{2+} + 4HCO_3^- \quad (13)$$

Anhydrite in dolostones undergoes a unique reaction:

$$CaSO_4 + CO_2 + H_2O \leftrightarrow CaCO_3 + H_2SO_4 \quad (14)$$

The rates of these reactions play a pivotal role in influencing the extent of changes to the petrophysical properties of carbonate rocks.[136] In formations containing a mixture of anhydrite, dolomite, and calcite, carbonic acid reacts more quickly with anhydrite and then with calcite compared to dolomite.[147] As a result, the impact of dissolution and other mechanisms like mechanical compaction and precipitation on dolomite rocks is expected to be less significant than on rocks in calcite formations.[136] This is because dolomites have two carbonate ions in their structure, whereas calcites have only one, requiring two moles of bicarbonates to dissolve one mole of dolomite but only one mole of bicarbonate to dissolve one mole of calcite.[148] Furthermore, Smith et al.[149] determined the reaction rate for calcite and dolomite to range from $10^{-6.8}$ to $10^{-4.8}$ and $10^{-7.8}$ to $10^{-5.3}$, respectively.

3.3. Factors Affecting the Dissolution Rate in Carbonate Minerals. Both calcite and dolomite dissolution rates are influenced by various factors, including CO_2 partial pressure, temperature, pH, salinity, among other factors.[150,151] These factors directly impact the chemical equilibrium and kinetics of the dissolution process, determining the extent and rate at which these carbonate minerals dissolve in carbonate reservoirs.

3.3.1. Temperature. Temperature plays a significant role in calcite and dolomite dissolution. Higher temperatures generally accelerate reaction rates. Peng et al.[152] observed higher dissolution rates of calcites as temperature increased from 50 to 100 °C. However, the impact of temperature on this process can be more complex[144] as Pokrovsky et al.[151] noted that at acidic pH, dissolution rates measured at 150 °C are equal or lower than dissolution rates at 100 °C, indicating a potential plateau or reversal of dissolution rate trends at increased temperatures.

3.3.2. Pressure. As CO_2 pressure increases, the pore fluid becomes more acidic due to the production of carbonic acid. This lowers the pH, which accelerates the dissolution of carbonate minerals. Luquot and Gouze[146] observed dissolution rates of 5.0×10^{-8} mol/cm^{2}s at a partial pressure of 25 bar. At a higher partial pressure of 100 bar in an experimental study by Menke et al.,[153] they observed even higher dissolution rates of

https://doi.org/10.1021/acs.energyfuels.4c04424
Energy Fuels 2025, 39, 1226−1251

Table 6. Summary of Previous Studies on the Effect of CO_2 on the Flow Properties of Carbonate Rocks

reference	objective(s)	methods	findings
		experimental studies	
161	investigate the effect of CO_2 during CO_2 flooding on carbonate rocks	core flood experiment	initial increase of permeability from 90.13 to 142.35md. However, subsequent mineral precipitation within the pore throats resulted in a reduction of permeability
162	investigate CO_2-brine-rock interactions at increased temperature and pressure	core flood experiment	dissolution of calcite and dolomitization increased porosity while precipitation of anhydrite reduced it.
164	quantifying coupled processes of mineral dissolution in aperture fractures	core flood experiment	porosity increased due to dissolution and later decreased due to mechanical compaction
147	determine the effects of pressure and CO_2 volume on the permeability of calcite cores	core flood experiment	permeability and porosity were decreased due to calcium carbonate precipitation
138	investigate the effect of temperature, pressure, and brine salinity on petrophysical changes during CO_2 storage.	solubility tests and core storage experiment	permeability and porosity decreased after a short storage time and then increased when storage time increased.
167	determine the effect of chalk-saturated water and CO_2-saturated solution on the mechanical strength of carbonates	conventional triaxial compression experiment	increased temperatures had no effect on the mechanical strength of carbonates, but the addition of pore fluid did
165	investigate the effect of CO_2 on porosity, permeability, and reactive surface area	core flood experiment	a range of dissolution patterns was observed, resulting in increased permeability
166	determine physical processes responsible for rock weakening	SEM and X-ray CT	strength in rocks is related to types of bonding between grains, which are affected by dissolution effects
149	use experimental data and 3D reactive transport models to predict the evolution of pore space and permeability	core flood experiment	heterogeneous limestone cores are predominantly affected by calcite dissolution due to its high reaction rate, while the slower reactivity of dolomite results in a slower development of porosity
159	investigate permeability alteration during CO_2 sequestration	helium porosity and brine permeability method	core permeability increased with higher injection pressures due to rock dissolution but decreased when temperature was increased from 27 to 100 °C
173	investigate the effect of CO_2 storage on permeability	triaxial seepage system	without the use of proppant, permeability decreased, but with proppant, permeability increased
		simulation studies	
168	study the physical and chemical impact of CO_2 injection on the properties of carbonates	TOUGH-REACT	weak reactivity with supercritical CO_2, hence less reservoir damage
146	study models of CO_2 injection and sequestration, and specifically the permeability/porosity scaling law	3D X-ray microtomography (XMT)	effective reaction area and porosity that control porosity are changed by dissolution
174	evaluate geochemical reactions and their effect on reservoir property	3D reactive simulation model	dissolution of dolomite can result in precipitation of calcite and ankerite
169	investigate the impact of CO_2-brine solution on carbonates at increased temperatures	COSMOL	increased temperatures led to mineral dissolution, thereby enhancing the rock permeability
175	investigate impact of pressure, well configuration, and contaminants on mineral trapping of CO_2	CMG	higher pressure and horizontal wells improve CO_2 trapping whiles impurities reduces the potential for mineral trapping of CO_2
171	investigate dolomitization and dissolution process of calcite	molecular dynamic simulation	calcite dissolves faster than dolomite, especially in acidic conditions
170	investigate the interactions between CO_2, brine, and aquifer minerals	PHREEQC	the precipitation of secondary minerals depends on Ca/Mg ratio present in the formation

https://doi.org/10.1021/acs.energyfuels.4c04424
Energy Fuels 2025, 39, 1226−1251

8.8×10^{-7} mol/cm^{2}s. Recently, Segura et al.[150] simulated the impact of low partial pressure (1 bar) and observed dissolution rates of 3.6×10^{-12} mol/cm^{2}s. This trend illustrates the direct relationship between increasing CO_2 pressure and enhanced dissolution rates.

3.3.3. Salinity. The salinity of the formation brine also affects dissolution rates. Generally, higher salinity levels lead to reduced CO_2 solubility, which in turn decreases the dissolution rate of carbonate minerals. Nomeli and Riaz[154] reported a decrease in dissolution rate of calcite as salinity increased. This was attributed to the decreased solubility of CO_2 at increased salinities. Similar results were observed by Gledhill and Morse[155] who noted that a decrease in dissolution rate as salinity increased. However, there are conflicting findings; Segura et al.[150] reported an increase dissolution rate as salinity increased, suggesting that additional mechanisms may be at play under certain conditions.

3.3.4. Other Influencing Factors. The acidity of the fluid is one of the most critical factors influencing the dissolution of carbonate minerals. Lower pH conditions promote dissolution by increasing the concentration of H^+ ions, which react with carbonate minerals to release divalent cations and bicarbonate ions (HCO_3^-). This process is evident in the increased dissolution rates of both calcite and dolomite under more acidic conditions.[146] Recent studies have shown that nanoparticles, particularly SiO_2, can enhance the dissolution of carbonate minerals. This enhancement is attributed to the increased dissolution of CO_2 in the brine in the presence of nanoparticles. Tan et al.[156] reported that the presence of SiO_2 nanoparticles increased the dissolution rate of calcite and dolomite, likely due to the nanoparticles' ability to alter surface reactions and improve CO_2 solubility in the brine.[157] Isah et al.[158] experimentally investigated the dissolution kinetics of anhydrite-rich rocks and the subsequent formation of minerals in the presence of CO_2 and varying brine concentrations. They introduced Strontium ions in the brine and observed that it strongly influenced the dissolution of the anhydrite surfaces.

Understanding these complex factors and their interdependencies is essential for predicting the behavior of dissolution rates in carbonate formations during CO_2 sequestration efforts. Further research is needed to clarify how salinity, impurities, and temperature interact in carbonate systems and to identify strategies for optimizing long-term CO_2 storage.

3.4. Impact of CO_2-Carbonate Reactions on Reservoir Flow Properties. Understanding the conditions that govern mineral dissolution and precipitation is crucial, as mineral dissolution enhances porosity and permeability[159] while precipitation of carbonate minerals significantly reduces these properties.[138] Unlike sandstone rocks, the relationship between permeability and porosity in carbonate rocks is complex. Specifically, carbonate reservoirs can exhibit a positive relationship between permeability and porosity, or they may have low permeability with high porosity, or vice versa.[160]

Several studies have investigated the impact of CO_2 injection on carbonate rocks (see Table 6). To demonstrate the effect of CO_2 on rocks, Luquot and Gouze[146] conducted experiments on limestone reservoir samples to study the impact of CO_2 on rocks. They found that high CO_2 partial pressure (10 MPa) created conductive flow channels, modifying permeability. Lower CO_2 partial pressure (6 and 2.5 MPa) resulted in controlled dissolution rates. At even lower CO_2 partial pressure (0.7 MPa), precipitation occurred, reducing porosity, and potentially clogging the medium. Omole and Osoba[161] conducted an experiment on dolomite cores, observing that at some distance away from the injection well, where the pressure drop was significant, there was a reduced concentration of CO_2, leading to the formation of insoluble carbonates. These precipitates caused pore throat restriction, thereby decreasing the permeability of the rock. At an increased temperature, Rosenbauer et al.[162] observed the kinetically rapid precipitation of anhydrite in an experimental study, resulting in scaling and a reduction in formation porosity during CO_2 injection.

In the experimental study conducted by Mohamed et al.[147] on limestone cores at 8.96 MPa and 93.33 °C, there was a reduction in permeability from 61.8 to 60.5 md, and porosity reduced from 0.196 to 0.182 due to the precipitation of calcium carbonate. A study on permeability alterations during CO_2 sequestration in an Iranian carbonate reservoir was carried out by Karaei et al.[159] The research involved varying injection pressures and temperatures at a confining pressure of 10 and 1 MPa. They observed that higher injection pressures increased core permeability as they enhanced rock dissolution, injectivity, and CO_2 solubility. Conversely, raising the temperature from 27 to 100 °C resulted in a reduced permeability, primarily because the conditions became less favorable for rock dissolution. In all cases, permeability was consistently lowest in formation brine conditions since salt precipitation takes place, which reduces formation permeability. These findings find support in the work of Adel and Shedid[138] where similar trends were identified. Their observations indicated that the porosity and permeability decreased when CO_2 was initially stored in a carbonate rock for a short period of time i.e., 7 days, but then these properties began to increase when CO_2 was stored for longer time intervals ($\geq$150 days).

Laboratory experiments on CO_2-water-rock interactions conducted by Cui et al.[163] on carbonate rock samples from the Tahe oilfield showed increased permeability and porosity after 40 years of exploitation. The permeability and porosity around the production well area increased from 0.02 to 0.021 md and 50 to 51.4 md, respectively. This was due to minerals dissolving in the reservoir. The increase in porosity, however, can cause the rock to weaken, and subsequent mechanical compaction can also cause porosity to reduce. This phenomenon was observed in a core flooding experiment by Detwiler.[164] After CO_2-charged brine was injected into dolomite cores at 100 °C and 15 MPa by Luhmann et al.,[165] a wide range of dissolution patterns were observed, which resulted in a significant increase in bulk permeability. Smith et al.[149] conducted a core-flood experiment at a temperature of 60 °C and confining pressure of 24.8 MPa on heterogeneous limestone cores and noted that they are primarily influenced by calcite dissolution, with faster-reacting calcite generating more porous spaces in the localized regions. An increase is porosity was observed during the dissolution of the limestone cores.

The mechanisms and processes behind the loss of rock strength due to water saturation in carbonate rocks have been investigated in experimental studies by Ciantia et al.[166] and Liteanu et al.[167] These processes were associated with the type of bonding between the rock particles, grain cracking, and pressure solution. In triaxial compression experiments conducted by Liteanu et al.,[167] chalk cores at temperature ranges of 20 to 80 °C and confining pressures up to 7 MPa showed that the increase in temperature did not significantly affect the strength of the samples. However, short-term weakening effects were observed due to the addition of water and CO_2-saturated fluid. Ciantia et al.[166] studied the behavior of soluble calcareous

https://doi.org/10.1021/acs.energyfuels.4c04424
Energy Fuels 2025, 39, 1226−1251

Table 7. Comparison of CO_2 Storage in Basalt vs. Carbonate Formations

aspect	basalt formations	carbonate formations
global distribution	volcanic regions	sedimentary basins
main minerals involved	olivine, pyroxenes, plagioclase, wollastonite, forsterite	dolomite, calcite, anhydrite, glauconite, phosphate, clays
reactivity with CO_2	highly reactive due to high concentrations of Ca^{2+}, Mg^{2+}, and Fe^{2+}, promoting rapid mineral carbonation	reactivity depends on mineral composition; calcite reacts faster than dolomite
mineral carbonate rate	fast; 2−10 years for majority of injected CO_2 to mineralize	slower; dissolution of minerals and subsequent precipitation occur over longer geological time scales
main carbon precipitates	calcite, magnesite, siderite, ankerite	calcite, dolomite, ankerite, siderite
impact on reservoir properties	increases porosity and permeability via dissolution but reduces via carbonate precipitation	heterogeneous, impacts are variable (can either increase or decrease porosity and permeability)

rocks from a microstructural perspective and found that the mechanism of strength loss or gain is related to the types of bonding between the rock particles, which are influenced by long-term dissolution effects.

Several simulation studies have been used to evaluate the effect of CO_2 injection on carbonate rocks. In a study by André et al.,[168] they considered two cases using a TOUGH-REACT code: one involving CO_2 in contact with saturated water and the other with CO_2 in a supercritical state at 75 °C. The simulation results, covering a 10-year injection period, showed significant reactivity with CO_2-saturated water, potentially leading to reservoir damage, while the reaction was weaker under supercritical CO_2 injection. In the first case, the high reactivity was associated with a porosity increasing up to 90%. To further characterize the behavior of carbonate rocks during CO_2 injection, a 3-D model was developed by Ben Mahmud et al.,[169] utilizing COMSOL Multiphysics software. Their findings, based on simulations at increased temperatures (up to 95 °C), indicated a slight increase in core plug volume, but a significant increase in permeability was due to the dissolution and dispersion of carbonate minerals. Al Salmi et al.[170] employed PHREEQC to investigate mineralogical changes in a carbonate aquifer and their impact on petrophysical properties. They observed that an increase in the volume fraction of calcite resulted in lower reaction rates, which reduced the mineral trapping efficiency of CO_2 and slowed porosity alteration. They also noted that the precipitation of secondary minerals depends on the availability of primary silicate minerals and the Ca/Mg ratio. They concluded that while PHREEQC is valuable for assessing geochemical reactions, reactive transport modeling is needed to account for more forces, such as multiphase flow. Zhu et al.[171] utilized molecular dynamic simulations (MDS) and density functional theory (DFT) calculations to investigate the dolomitization and dissolution processes of carbonate minerals. They found that calcite dissolves faster than dolomite, especially under acidic conditions induced by CO_2 injection, while dolomite remains relatively stable due to its slower dissolution rate. In another simulation study, Bello et al.[172] used CMG software to investigate CO_2 mineral trapping mechanisms in saline aquifers. Their results indicated that calcite and dolomite mineralize more efficiently at medium to lower temperatures. However, as salinity increases, the trapping efficiency decreases because increased ionic strength leads to higher water viscosity, slowing CO_2 propagation.

Despite these numerical and experimental studies, the underlying mechanisms controlling these mineral dissolutions and precipitation are not yet fully understood. Critical areas requiring further research include the specific geochemical conditions that promote or inhibit changes in permeability and porosity, the differential behaviors of calcite and dolomite in response to CO_2 exposure, and the long-term stability of carbonate formations under varying temperatures and pressures. Advancing our understanding in these areas will significantly improve the predictability and efficiency of CO_2 sequestration techniques, contributing to climate change mitigation.

4. OPTIMIZATION OF CARBON MINERALIZATION

In Table 7, the key differences between CO_2 storage in basalt and carbonate formations are highlighted, showing that basalt formations emerge as the superior option for CO_2 storage. This is primarily due to the rapid mineral carbonation process in basalts. The minerals in basalts are rich in divalent cations which react quickly with dissolved CO_2 to form stable carbonate minerals.[129,176] Additionally, the widespread availability of basalts and their rapid trapping mechanisms make them the most efficient and reliable choice for long-term CO_2 storage.

To fully leverage the advantages of basalt formations, optimization of CO_2 mineralization is important. There are several factors that can enhance the efficiency of CO_2 trapping mechanisms including temperature, pressure, salinity, presence of impurities, and availability of divalent cations.

It has been shown in the literature that higher temperatures significantly accelerate the dissolution rates of the minerals. There is faster cation release, which enhances the carbonation process. Optimal sites considered for storage should ideally be deeper formations with natural geothermal gradients that ensure higher temperatures. In addition, the partial pressure of CO_2 and the pressure of the system plays a critical role in reducing the pH of the environment, which facilitates the release of cations from basalt minerals for their subsequent precipitation with CO_2. Unaltered basalts exhibit faster mineralization rates than altered ones, making sites with high proportions of unaltered basalts ideal for CO_2 storage.

Low salinity levels also promote the dissolution of CO_2 and minerals, further enhancing the carbonation process. Injecting CO_2 with impurities like H_2S and/or other impurities reduces costs and increases the reactivity of the basalt, thereby enhancing CO_2 mineralization potential. Additionally, the use of nanoparticles and organic ligands can further promote mineralization by modifying fluid-rock interactions. By carefully selecting storage sites and optimizing injection conditions, the efficiency of CO_2 mineralization in basalt formations can be significantly enhanced, providing a sustainable and cost-effective solution for mitigating climate change.

https://doi.org/10.1021/acs.energyfuels.4c04424
Energy Fuels 2025, 39, 1226−1251

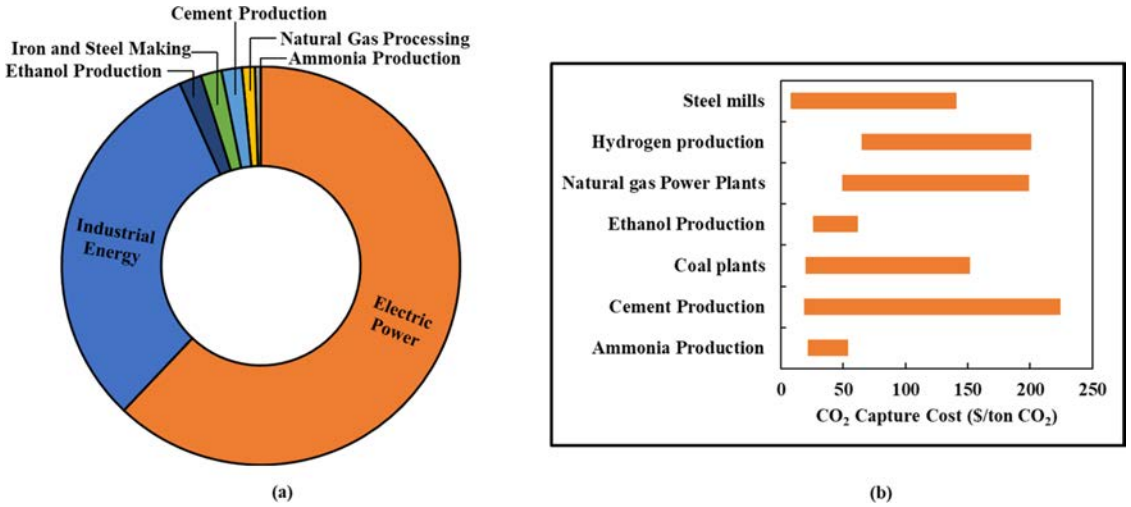

Figure 10. (a) Emission sources of CO_2 from various industries.[10] (b) Estimates of CO_2 Capture costs by industry, presented in 2021 U.S. dollars.[180]

5. TECHNO-ECONOMIC CHALLENGES OF CCS IN BASALTIC AND CARBONATE RESERVOIRS

Although basaltic and carbonate formations offer unique opportunities for CO_2 storage, the effectiveness and viability of CCS projects within these formations depend on various factors. These include the cost associated with implementation, injectivity rates of CO_2, secure containment of the injected CO_2, and monitoring technologies to ensure environmental safety. Each of these factors is discussed in detail below.

5.1. Cost Analysis. Despite its role in achieving clean energy transitions, the global deployment of CCS technologies in these formation types has been slow to gain momentum. Several factors contribute to this slow uptake, with cost being a significant hurdle. Numerous studies have investigated the costs associated with CCS technologies,[177,178] which encompasses the costs related to capturing, transporting, and the geological storage of CO_2.

5.1.1. CO_2 Capture. The primary sources of CO_2 currently are from various industrial sources and electricity power generation (see Figure 10a). Given the significant role that these sources play in contributing to greenhouse gas levels, capturing CO_2 from these emissions is important. High-purity sources, such as natural gas and ethanol processing plants, produce CO_2 streams that contain over 90% CO_2 by volume with minimal other impurities.[179] These sources are generally characterized by lower capture costs because their CO_2 streams are already close to pipeline transport standards. In contrast, low-purity sources like cement plants produce CO_2 streams with a lower concentration of CO_2 and higher levels of other gases.[10,179] As a result, capturing CO_2 from these sources incurs additional costs to increase CO_2 concentration and remove other impurities to comply with pipeline standards. It is important to note that while the cost of capturing CO_2 is important, it only accounts for the capture process itself and does not include additional expenses of transporting and storing the captured CO_2.[177]

Various technological pathways exist for CO_2 capture, each with different costs and efficiencies. They include precombustion, postcombustion, industrial separation, chemical looping, and oxy-fuel combustion.[181] Table 8 provides a summary of the capture rates and associated costs for these different technologies, while Figure 10b illustrates the estimated cost range for capturing a metric ton of CO_2 from the different CO_2-emitting sources. Precombustion technologies achieve a capture rate of 90−97.3% at a cost of around $60 per ton of CO_2, while postcombustion technologies capture 90−99% of CO_2 at a cost ranging from $46 to $74 per ton.[182−185] Industrial separation and chemical looping also offer competitive capture rates and costs, with oxy-fuel combustion being another viable option. In addition to these traditional methods, direct air capture (DAC) has emerged as a promising new technology. Recent advancements have significantly reduced DAC costs, with estimates ranging from $135−$345/ton CO_2, although some projections suggest cost could still reach $600−$1000 per ton in the near future due to various implementation factors.[10] These variations in CO_2 capture costs are primarily due to differences in the CO_2 concentration and pressure in the pipelines.[10] Higher CO_2 concentration and pressure generally result in lower capture costs for a given amount of CO_2.[10]

Table 8. CO_2 Capture Rate and Costs of Different Capture Technologies

reference	capture technology	CO_2 capture rate (%)	cost range ($/ton CO_2)
182,183	pre-combustion	90−97.3	60
184,185	post-combustion	90−99	46−74
186	industrial separation	90	34.8−60.9
187	chemical looping	98.5	40−74
188,189	oxy-combustion	90	45−66
10,190,191	direct air capture	85−93	135−1000

While these capture technologies are effective, their high costs pose a significant barrier to the large-scale deployment of carbon capture and storage (CCS). Continued research and innovation in capture technology, as well as economies of scale, will be key to driving down costs and enabling broader adoption. By addressing this, it may become feasible to capture and sequester carbon at the scale needed to meet global climate goals.

5.1.2. CO_2 Transportation. Postcapture, CO_2 is purified and compressed into a concentrated, pressurized liquid for pipeline transportation to storage sites. The transportation cost of captured CO_2 is influenced by the volume being transported, the distance to be covered, and the loading capacity of the vessel.[192] There are various methods for transporting CO_2, such as ships, road tankers, pipelines, and rail tankers.[193] Among these, pipeline transportation is widely recognized as the most

https://doi.org/10.1021/acs.energyfuels.4c04424
Energy Fuels 2025, 39, 1226−1251

economical option, especially for large volumes of CO_2[194] with over 5000 miles of pipelines used in the U.S.A.[195] The efficiency of gas movement through pipelines is primarily dependent on pressure, as gases naturally flow from high-pressure areas to low-pressure areas, ensuring a continuous and efficient transport process.

The costs involved with transportation comprise three main components: operation costs, construction costs (i.e., labor and material), and maintenance costs (including design and monitoring).[1] Cost estimates are typically model-based. Costs also depend significantly on the terrain through which the pipeline is routed. Onshore pipeline costs can rise by 50 to 100% or more when the route traverses heavily populated or congested areas. Offshore pipelines, which typically operate at lower temperatures and higher pressures than onshore pipelines, tend to be even more expensive—often by 40 to 70%—due to the additional technical challenges and environmental considerations involved.[196] As illustrated in Figure 11, the costs

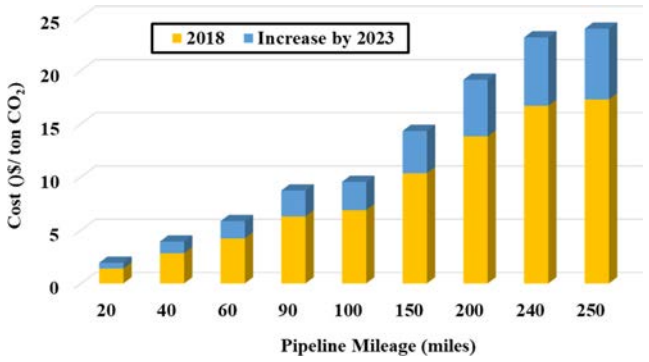

Figure 11. Pipeline transportation cost comparison (2018 vs 2023).[178]

associated with pipeline transportation have been reported to be increasing over time, primarily driven by rising material costs and stricter environmental regulations. To optimize costs, several strategies can be employed including, leveraging economies of scale, optimal pipeline design, and route optimization. Economies of scale allow for reduced unit costs as pipeline capacities grow, while optimal design considerations—such as pipe diameter and material selection—can further enhance cost efficiency, ensuring a more cost-effective transportation system for CCS projects.[37,185]

5.1.3. CO_2 Storage. The geological storage costs of CO_2 are affected by various factors, including the geological characteristics of the subsurface formation, the amount of CO_2 to be stored, and the associated monitoring, financial, and modeling assumptions.[197] Specifically, these costs are closely tied to the reservoir type—such as sedimentary formations, basalt formations, and others—as well as the reservoir petrophysical properties, the number of injection wells, the flow rate, and the storage method employed, all of which play a significant role in determining the overall feasibility and cost-effectiveness of CO_2 storage.[13,22] Similar to the transportation costs associated with pipelines, offshore CO_2 storage tends to be more expensive than onshore CO_2 storage.[198]

Table 9 provides a summary of the costs associated with CO_2 storage in basaltic and sedimentary formations. As shown in Table 9 while mineralization occurs more rapidly in basaltic formations, the associated storage costs are higher. In contrast, sedimentary formations, which are typically porous and permeable, require fewer injection wells, making them more

Table 9. CO_2 Storage Cost Range in Storage Formations[178,199]

storage formation	cost range ($/ton CO_2)
basalt formation	20−30
sedimentary formations	6−14.85

cost-effective. This highlights the importance of a comprehensive comparison of operating costs across different formations to identify the most economically viable options.

The high costs of CCS make it uncompetitive for integration with existing facilities and widespread adoption in other regions. However, in the U.S.A., the 45Q tax credit was introduced under the Energy Improvement and Extension Act of 2008, providing capture operators a credit for each ton of CO_2 stored or utilized. This incentive has been significantly expanded by the Inflation Reduction Act (IRA) of 2022, which substantially raised the value of tax credits by 70% to $85 per ton of CO_2 captured and stored from industrial facilities and power plants, and by 250% to $180 per ton of CO_2 for direct air capture facilities.[11,200] Additionally, the IRA introduced options for monetization, such as credit transfers to third parties or direct payments from the Treasury, relaxed annual thresholds for facility qualification, and extended the start date on eligible projects from 2026 to 2033.

Despite these enhanced incentives, the 45Q tax credit alone does not sufficiently offset the total costs involved with CCS projects, particularly in the power generation sector, making it economically unviable.[180] However, the IRA's provisions are expected to significantly boost the number of CCS projects entering the service in the coming years, potentially increasing global capture capacity of CO_2.

As CCS costs typically decrease with larger-scale projects, the development of CCS hubs—centralized locations for CO_2 collection and distribution—has emerged as a strategy to reduce these costs.[197,201] Potential hubs in the U.S.A., such as those in Wyoming, the Texas and Louisiana Gulf Coast, and the Ohio River Valley, aim to streamline operations and enhance economic viability. Nevertheless, the path forward for large-scale CCS deployment will require not only continued technological advancements but also more substantial economic incentives and policy support to overcome these significant techno-economic barriers.

5.2. Injectivity of CO_2. Injectivity, also known as well capacity, refers to the ease with which fluid can be injected into storage media without causing the creation of new fractures or reactivating existing faults near the wellbore.[202] It governs the long-term safety of CCS projects. The injectivity is affected by factors such as formation permeability, porosity, and thickness.[203] For favorable injectivity, there must be high permeability in the near-wellbore region.[204] The injection of CO_2 in basalt and carbonate formations, however, leads to permeability and porosity alterations, which affects the injectivity. Numerous studies have investigated injectivity in basalt and carbonate formations,[40,205,206] finding that during the injection of CO_2, mineral dissolution improves the flow properties of the near well-bore region, while mineral precipitation negatively impacts the flow properties of the reservoir. In basalts, since the goal is to achieve mineral carbonation in the short term, a high injection rate is usually employed.[207] This, however, could reduce the permeability and porosity in the near-wellbore region, and as such, further research is needed to clarify optimum injection rates into basaltic formations while having minimal impact on the flow

https://doi.org/10.1021/acs.energyfuels.4c04424
Energy Fuels 2025, 39, 1226−1251

Table 10. Framework for Addressing Gaps, Challenges, and Future Risks in Basaltic and Carbonate Reservoirs

category	gaps/challenges	future risks	recommendations
cost	• high upfront and operational costs	• financial barriers to widespread adoption	• diversify funding sources
	• variability in costs based on source, concentration, and pressure of CO_2		• develop cost-effective technologies, e.g., CCS hubs.
injectivity	• alterations in permeability and porosity	• reduced injectivity over time	• conduct large-scale studies to determine optimum injection rates
	• lack of comprehensive research on optimum injection rates	• wellbore damage	• develop advanced characterization techniques for accurate reservoir modeling
storage	• uncertainty about the long-term stability of CO_2 in storage media	• health and safety concerns related to groundwater contamination	• improve site selection techniques and enhance monitoring systems
	• potential for CO_2 leakage and groundwater contamination		• develop robust reactive transport models to predict CO_2 plume behavior
monitoring	• limited application/use of advanced monitoring methods and technology in storage media	• inadequate detection of CO_2 leakages	• invest in advanced sensors and analytics
		• inconsistent monitoring data	• establish standardized monitoring protocols
research and development	• limited understanding of long-term geochemical interactions between CO_2 and these formations	• technological limitations in prediction and modeling	• conduct more pilot studies and large-scale field experiments
public acceptance	• lack of awareness of CCS technologies and negative perceptions	• social opposition to CCS projects	• engage with communities to build public acceptance

properties of the reservoir. While there has been significant focus on CO_2-EOR applications in carbonate formations, which hold about 60% of global hydrocarbons,[139,208,209] comprehensive studies on CO_2 injectivity in carbonate reservoirs remain limited. Addressing these knowledge gaps is crucial for effectively utilizing these formations for CO_2 storage.

5.3. Containment and Integrity of Injected CO_2. Containment of CO_2 depends on overlying caprocks and any faults or fractures within them.[210] The sealing potential of the caprock is the most significant aspect of the containment of CO_2. In carbonate formations, CO_2-water-rock interactions affect the sealing efficiency of caprocks, leading to alterations in permeability and porosity that can cause CO_2 leakage.[211] These alterations, however, are very slow, and their effects are, therefore, very hard to quantify within the time span of laboratory experiments.[212,213] Further research is needed to securely trap CO_2 in carbonate formations effectively.

Unlike carbonate formations, basaltic formations have distinct geological characteristics that influence CO_2 containment and integrity. Basalts, formed from volcanic activity, generally lack caprocks, which are typically present in carbonate formations. Instead, basalts may contain natural fractures resulting from the cooling and solidification of lava.[63] Despite the presence of these fractures, the dense structure of basalts tends to restrict CO_2 migration through these fractures, thereby enhancing the potential for CO_2 trapping within the reservoir. Studies have shown that CO_2 migration in basalts is influenced by intrinsic permeability, retention properties, and formation stratigraphy.[214] The presence of CO_2 can lead to interactions between rock and water, potentially altering fracture structures. Further research is crucial to understand the integrity of injected CO_2 in basalts.

The containment and integrity of injected CO_2 are very critical because leakage of CO_2 can lead to groundwater contamination.[129] The International Energy Agency (IEA) developed a comprehensive framework for risk assessment, management, and communication in CO_2 sequestration projects to address this challenge. It also outlines a structured approach involving planning, implementation, and monitoring activities to ensure the safe operation of CCS projects.[22] This framework consists of three core stages: risk assessment, exposure assessment, and risk management. The risk assessment stage includes site selection and characterization, followed by risk identification and vulnerability assessment to identify potential risks associated with the storage site. The exposure assessment stage focuses on detailed site characterization, simulating the storage complex, and evaluating security, sensitivity, and hazards, followed by effect assessment and risk characterization to understand potential exposure risks and the impact of CO_2 storage. In the final stage, risk management, the framework emphasizes risk evaluation, treatment, and ongoing monitoring and verification to ensure the site's long-term safety.[215]

5.4. Monitoring Techniques. The long-term storage of CO_2 in basalt formations and carbonate formations requires a suitable monitoring technique. Monitoring techniques help detect and quantify possible leakages. There are several methods that are frequently employed, including acoustic and seismic monitoring, in-well pressure and temperature monitoring, chemical and oceanographic monitoring, geochemical sampling, remote sensing, and gravimetric monitoring.[216−218] Most of these monitoring techniques are used in sedimentary formations, and due to their success stories, they are being applied to monitor CO_2 storage in basalt formations.[40] However, alternative monitoring methods have been proposed specifically for storage in basalt formations. Khatiwada et al.[219] investigated the potential of scattered seismic waves to remotely sense the sequestration of CO_2 in basalts. Their results showed that scattered seismic waves in layered earth models like basalts are sensitive to velocity perturbations and can monitor the reservoir's physical changes. Matter et al.[220] developed a reactive tracer technique to monitor and detect both dissolved and mineralized CO_2. The method involves tagging the injected CO_2 with low levels of radiocarbon (^{14}C) as a reactive tracer. This method was applied at the CarbFix pilot injection, and the precipitation of minerals in the basalt formation was successfully calculated. Recently, Bartels et al.[221] developed a thermogravimetric analysis-mass spectrometry (TGA-MS) technique to quantify calcite precipitates in complex samples. Applied to a suite of Columbia River Basalt Group samples, this method indicated average carbonate contents of 0.05 wt % in the flow interiors (caprock) and 0.4 wt % in the reservoir, demonstrating its effectiveness in monitoring mineral precipitation in basalt

https://doi.org/10.1021/acs.energyfuels.4c04424
Energy Fuels 2025, 39, 1226−1251

formations. Wang et al.,[222] however, noted that this method could involve cumbersome steps, and conducted a self-designed high temperature and high-pressure reactor experiment and quantified the mineralization efficiency by combining pressure data with a numerical model, expressed below in eq 15.

$$\mathrm{CSE} = \frac{(n_1 - n_m) \times M_{\mathrm{CO_2}}}{M_{\mathrm{B}} \times \mathrm{CSP}} \times 100 \tag{15}$$

Where CSE is the carbon sequestration efficiency, %, $M_{\mathrm{CO_2}}$ is the molecular mass of CO_2, the basalt mass is denoted by M_{B}, $n_{(1,2...m)}$ is the amount of matter at different times of CO_2, and CSP is the carbon sequestration potential, expressed in eq 16.

$$\mathrm{CSP} = \left(\frac{W_{\mathrm{Ca}}}{M_{\mathrm{Ca}}} + \frac{W_{\mathrm{Mg}}}{M_{\mathrm{Mg}}} + \frac{W_{\mathrm{Fe}}}{M_{\mathrm{Fe}}}\right) \times M_{\mathrm{CO_2}} \tag{16}$$

where $W_{(\mathrm{Ca,\ Mg,\ Fe})}$ and $M_{(\mathrm{Ca,\ Mg,\ Fe})}$ are the mass percentages and molar masses of Ca, Mg, and Fe in the basalt samples, respectively.

For sedimentary formations, Fawad and Mondol[223] used a new rock physics model to facilitate the time-lapse estimation of pressure changes within the reservoir based on the physical properties of the reservoir obtained from prestack seismic inversion.

However, to further enhance monitoring techniques, it is crucial to incorporate advanced technologies like autonomous and remotely operated vehicles, ships, and sensors. These advanced technologies will be crucial in enhancing our monitoring techniques and ensuring the safe and efficient storage of CO_2.

6. CHALLENGES AND FUTURE OUTLOOK

This comprehensive review of CO_2 mineralization in carbonate and basalt formations highlights promising pathways for CO_2 sequestration yet reveals several areas requiring further investigation and development (see Table 10). This section highlights the key challenges, research gaps, future perspectives in this field, and potential advancements in research methodologies.

One of the key challenges in CO_2 sequestration lies in maintaining injectivity over time while optimizing mineralization rates. Although basalt formations offer faster CO_2 mineralization compared to other geological formations, a critical issue that arises during CO_2 injection is the reduction in injectivity over time due to mineral precipitation, which may clog pore spaces and decrease permeability, potentially limiting the formation's ability to accept further CO_2 injection. There is still limited understanding of the optimal conditions, such as temperature, pressure, and pH, that can accelerate mineralization while maintaining the structural integrity of the storage site. Another major obstacle is the heterogeneous nature of both basalt and carbonate formations, which significantly affects flow dynamics and reaction rates. This is especially evident in carbonate formations, where permeability and porosity can vary widely, making it difficult to predict CO_2 trapping mechanisms. Improved predictability and optimized injection strategies require a deeper understanding of how these variations influence the process. Additionally, ensuring the long-term integrity of caprocks is crucial for the secure storage of CO_2. Caprocks can be compromised by physical, chemical, or mechanical degradation during injection, particularly when impurities are present in the CO_2 stream. More research is needed to fully understand how these interactions between caprocks, the reservoir, and CO_2 under varying conditions could potentially threaten the long-term security of CO_2 storage.

Research gaps also exist concerning the long-term geochemical interactions between CO_2 and these formations. While pilot studies have shown promise for rapid mineralization in basalts, the long-term stability of these minerals and potential for leakage over geological time scales need further investigation. Similarly, the impact of CO_2 injection on the mechanical properties of basalts and carbonates, including the potential for induced seismicity, requires thorough evaluation. One major gap is the lack of detailed studies on postmineralization behavior over extended time scales, particularly under fluctuating environmental conditions like temperature and pressure. Additionally, most research has been conducted on a laboratory or small scale, making field-scale CO_2 injection experiments essential to validate these findings and ensure consistent results across different geological formations. Lastly, advancing numerical modeling and simulation tools is crucial. While tools like TOUGH-REACT, COMSOL, CrunchTope, CMG, etc. have been useful, more comprehensive models that integrate geochemical, hydrological, and mechanical factors are needed, along with machine learning approaches to enhance prediction accuracy for CO_2 behavior in complex, heterogeneous formations.

Future research should focus on addressing these challenges and knowledge gaps. Large-scale field studies with comprehensive monitoring programs are essential to validate laboratory findings and assess the long-term viability of CO_2 storage in these formations. The development of robust reactive transport models, incorporating detailed characterization data and accounting for complexities like heterogeneity, will be crucial for predicting CO_2 plume behavior and optimizing injection strategies. Moreover, economic considerations and the development of cost-effective CO_2 capture and injection technologies are essential for the widespread adoption of CO_2 storage in carbonate and basaltic formations. To enhance mineralization efficiency, future work should explore enhanced mineralization techniques, such as pretreating CO_2 with additives like organic ligands or nanoparticles, which have shown potential in accelerating mineral dissolution. Additionally, integrating machine learning into research can significantly improve the prediction of CO_2 interactions with brine and reservoir rocks. AI-driven models that process large data sets from field-scale experiments can enhance the accuracy of simulations and predictions, thus optimizing storage performance. Further research is also needed on CO_2 injection into altered basalts, as these formations may respond differently compared to fresh basalts. Understanding their reactivity will expand the number of viable storage sites. Finally, advancements in experimental and monitoring methods are crucial for real-time observation of CO_2-mineral reactions. In-situ testing tools and innovative tracer techniques can improve understanding mineral precipitation and dissolution dynamics and track CO_2 migration through rock formations more effectively. By addressing these challenges and pursuing further research, these formations have the potential to play a significant role in mitigating climate change through effective and secure CO_2 storage.

7. CONCLUSIONS

This comprehensive review examines CO_2 sequestration within basaltic and carbonate formations, focusing on the underlying trapping mechanisms, key influencing factors, and recent

https://doi.org/10.1021/acs.energyfuels.4c04424
Energy Fuels 2025, 39, 1226−1251

advances in both experimental and numerical studies. The following conclusions summarize the critical findings from our review:

- Basaltic formations exhibit significant potential for rapid CO_2 mineralization, particularly due to their high reactivity and abundance of divalent cations, making them ideal for CCS as opposed to carbonate formations, where the mineralization process may take significantly longer.
- Factors such as pressure, temperature, salinity, and pH significantly impact mineralization rates. High temperatures and CO_2 partial pressures accelerate the dissolution of basaltic minerals, enhancing carbonate precipitation. However, the exact impact of system pressure on dissolution rates remains unclear, requiring further investigation.
- In order to optimize CO_2 mineralization in basalt formations, CO_2 should be injected into deeper formations with natural geothermal gradients that ensure higher temperatures. Additionally, pretreating CO_2 with nanoparticles and organic ligands can aid in enhancing CO_2 mineralization.
- Numerical models are essential for predicting CO_2 behavior, but they need refinement to capture complex geochemical, hydrological, and mechanical interactions. Integrating machine learning techniques enhances prediction accuracy and optimizes CO_2 storage strategies.
- Advancing monitoring tools are vital to track CO_2-mineral interactions in real time to improve the predictability of mineralization rates and ensure the integrity of CO_2 storage sites. Experimental methods that simulate field-scale conditions will help bridge the gap between laboratory research and practical applications.
- The high cost of CCS remains a significant barrier to widespread implementation, with costs varying across capture, purification, transport, and storage phases. Widespread adoption for large-scale CCS deployment demands not only continued technological advancements but also more substantial economic incentives and supportive policies.
- The containment of CO_2 relies on the integrity of caprocks in carbonates and the dense structure of basalts, with challenges such as mineral reactions, fracture networks, and caprock integrity. Addressing these issues require careful site selection, risk assessment, and continuous monitoring.

AUTHOR INFORMATION

Corresponding Author

Aaditya Khanal − *Russell School of Chemical Engineering, The University of Tulsa, Tulsa, Oklahoma 74104, United States; McDougall School of Petroleum Engineering, The University of Tulsa, Tulsa, Oklahoma 74104, United States;* orcid.org/0000-0003-1333-7457; Email: aaditya-khanal@utulsa.edu, aadityakhanal@gmail.com

Authors

Prince N. Y. M. Otabir − *Russell School of Chemical Engineering, The University of Tulsa, Tulsa, Oklahoma 74104, United States*

Fatick Nath − *School of Engineering, Petroleum Engineering Program, Texas A&M International University, Laredo, Texas 78041, United States*

Complete contact information is available at: https://pubs.acs.org/10.1021/acs.energyfuels.4c04424

Author Contributions

P.O.: Conceptualization, investigation, formal analysis, resources, data curation, writing—original draft, writing—review and editing, visualization. A.K.: Conceptualization, validation, writing—review and editing, formal analysis, resources, funding acquisition, supervision, project administration. F.N.: Validation, formal analysis, investigation, resources, writing—review and editing. All authors have read and agreed to the publishing of the manuscript.

Notes

The authors declare no competing financial interest.

ACKNOWLEDGMENTS

We are grateful to the anonymous reviewers for their valuable edits and suggestions, which have significantly enhanced our manuscript. This material is based upon work partly supported by the National Science Foundation Award under CBET2245484. Any opinions, findings, and conclusions or recommendations expressed in this material are those of the author(s) and do not necessarily reflect the views of the National Science Foundation.

REFERENCES

(1) Ang, L.; Yongming, L.; Xi, C.; Zhongyi, Z.; Yu, P. Review of CO2 Sequestration Mechanism in Saline Aquifers. *Nat. Gas Ind. B* **2022**, *9* (4), 383−393.

(2) Al-Ghussain, L. Global Warming: Review on Driving Forces and Mitigation. In *Environmental Progress and Sustainable Energy*; John Wiley and Sons Inc., January 1, 2019; pp 13−21 DOI: 10.1002/ep.13041.

(3) U.S. Energy Information Administration. Where Greenhouse Gases Come From. https://www.eia.gov/energyexplained/energy-and-the-environment/where-greenhouse-gases-come-from.php According to EPA in 2021, emissions in the United States. (accessed 2024−09−10).

(4) Gyimah, E.; Tomomewo, O.; Nkok, L. Y.; Bade, S. O.; Ofosu, E. A.; Bawuah, M. C. A Probabilistic Study of CO2 Plume Geothermal and Hydrothermal Systems: A Sensitivity Study of Different Reservoir Conditions in Williston Basin, North Dakota. *Eng* **2024**, *5* (3), 1407−1421.

(5) National Centers for Environmental Information. Billion-Dollar Weather and Climate Disasters. National Oceanic and Atmospheric Administration. https://www.ncei.noaa.gov/access/billions/ (accessed 2023−01−06).

(6) Thonemann, N.; Zacharopoulos, L.; Fromme, F.; Nühlen, J. Environmental Impacts of Carbon Capture and Utilization by Mineral Carbonation: A Systematic Literature Review and Meta Life Cycle Assessment. *J. Cleaner Prod.* **2022**, *332*, No. 130067.

(7) United Nations Framework Convention on Climate Change. Summary of global climate action at COP28. https://unfccc.int/sites/default/files/resource/Summary_GCA_COP28.pdf (accessed 2024−02−07).

(8) Benson, S. M.; Cole, D. R. CO2 Sequestration in Deep Sedimentary Formations. *Elements* **2008**, *4* (5), 325−331.

(9) Zhu, Q. Developments on CO2-Utilization Technologies. *Clean Energy*; Oxford University Press May 25, 2019; pp 85−100. DOI: 10.1093/ce/zkz008.

(10) Congressional Budget Office. Carbon Capture and Storage in the United States. https://www.cbo.gov/system/files/2023-12/59345-carbon-capture-storage.pdf (accessed 2024−02−07).

(11) Global CCS Institute. Collaborating for a net zero future. https://www.globalccsinstitute.com/wp-content/uploads/2024/10/2024-GSR_20241015.pdf (accessed 2024−07−11).

(12) Nghiem, L.; Shrivastava, V.; Kohse, B.; Hassam, M.; Yang, C. Simulation of Trapping Processes for CO2 Storage in Saline Aquifers. In *Canadian International Petroleum Conference*; Petroleum Society of Canada, 2009 DOI: 10.2118/2009-156.
(13) Kumar, S.; Foroozesh, J.; Edlmann, K.; Rezk, M. G.; Lim, C. Y. A Comprehensive Review of Value-Added CO2 Sequestration in Subsurface Saline Aquifers. *J. Nat. Gas Sci. Eng.* **2020**, *81*, No. 103437, DOI: 10.1016/j.jngse.2020.103437.
(14) Memon, S. U. R.; Manzoor, R.; Fatima, A.; Javed, F.; Zainab, A.; Ali, L.; Ullah, U.; Saleem, A.; Ullah, Q. A Comprehensive Review of Carbon Capture, Utilization, and Storage (CCUS): Technological Advances, Environmental Impact, and Economic Feasibility. *Sch. Acad. J. Biosci.* **2024**, *12* (07), 184−204.
(15) Rasool, M. H.; Ahmad, M.; Ayoub, M. Selecting Geological Formations for CO2 Storage: A Comparative Rating System. *Sustainability* **2023**, *15* (8), 6599.
(16) Shukla, R.; Ranjith, P.; Haque, A.; Choi, X. A Review of Studies on CO2 Sequestration and Caprock Integrity. *Fuel* **2010**, *89* (10), 2651−2664, DOI: 10.1016/j.fuel.2010.05.012.
(17) De Silva, G. P. D.; Ranjith, P. G. G.; Perera, M. S. A. Geochemical Aspects of CO2 Sequestration in Deep Saline Aquifers: A Review. *Fuel* **2015**, *155*, 128−143.
(18) Zhang, D.; Song, J. Mechanisms for Geological Carbon Sequestration. *Procedia IUTAM* **2014**, *10*, 319−327.
(19) Shahriar, M. F.; Khanal, A. Effect of Formation Heterogeneity on CO2 Dissolution in Subsurface Porous Media. *ACS Earth Space Chem.* **2023**, *7* (10), 2073−2090.
(20) Ali, M.; Jha, N. K.; Pal, N.; Keshavarz, A.; Hoteit, H.; Sarmadivaleh, M. Recent Advances in Carbon Dioxide Geological Storage, Experimental Procedures, Influencing Parameters, and Future Outlook. *Earth-Sci. Rev.* **2022**, *225* (December 2021), No. 103895.
(21) Askarova, A.; Mukhametdinova, A.; Markovic, S.; Khayrullina, G.; Afanasev, P.; Popov, E.; Mukhina, E. An Overview of Geological CO2 Sequestration in Oil and Gas Reservoirs. *Energies* **2023**, *16* (6), 2821.
(22) Luo, J.; Xie, Y.; Hou, M. Z.; Xiong, Y.; Wu, X.; Lüddeke, C. T.; Huang, L. Advances in Subsea Carbon Dioxide Utilization and Storage. *Energy Rev.* **2023**, *2* (1), No. 100016.
(23) Liang, Y.; Tsuji, S.; Jia, J.; Tsuji, T.; Matsuoka, T. Modeling CO2-Water-Mineral Wettability and Mineralization for Carbon Geo-sequestration. *Acc. Chem. Res.* **2017**, *50* (7), 1530−1540.
(24) Li, Y. H.; Shen, C. H.; Wu, C. Y.; Hsieh, B. Z. Numerical Study of CO2 Geological Storage in Saline Aquifers without the Risk of Leakage. *Energies* **2020**, *13* (20), 5259 DOI: 10.3390/en13205259.
(25) Suekane, T.; Nobuso, T.; Hirai, S.; Kiyota, M. Geological Storage of Carbon Dioxide by Residual Gas and Solubility Trapping. *Int. J. Greenhouse Gas Control* **2008**, *2* (1), 58−64.
(26) Bachu, S. CO2 Storage in Geological Media: Role, Means, Status and Barriers to Deployment. *Prog. Energy Combust. Sci.* **2008**, *34*, 254−273.
(27) Pruess, K.; Spycher, N. ECO2N - A Fluid Property Module for the TOUGH2 Code for Studies of CO2 Storage in Saline Aquifers. *Energy Convers. Manage.* **2007**, *48* (6), 1761−1767.
(28) Mosavat, N.; Abedini, A.; Torabi, F. Phase Behaviour of CO2-Brine and CO2-Oil Systems for CO2 Storage and Enhanced Oil Recovery: Experimental Studies. *Energy Procedia* **2014**, *63*, 5631−5645.
(29) Ghanbari, S.; Pickup, G. E.; Mackay, E.; Gozalpour, F.; Todd, A. C. Simulation of Co 2 Storage in Saline Aquifers. 2006, No. September, 764−775. DOI: 10.1205/cherd06007.
(30) Sengul, M. CO2 Sequestration—A Safe Transition Technology. In *SPE International Health, Safety & Environment Conference*; SPE, 2006 DOI: 10.2118/98617-MS.
(31) Ibrahim, M. H.; El-Naas, M. H.; Benamor, A.; Al-Sobhi, S. S.; Zhang, Z. Carbon Mineralization by Reaction with Steel-Making Waste: A Review. *Processes* **2019**, *7* (2), 115 DOI: 10.3390/pr7020115.
(32) Siqueira, T. A.; Iglesias, R. S.; Ketzer, J. M. Carbon Dioxide Injection in Carbonate Reservoirs − a Review of CO2-Water-Rock Interaction Studies. *Greenhouse Gases: Sci. Technol.* **2017**, *7* (5), 802−816.
(33) Gysi, A. P. Numerical Simulations of CO2 Sequestration in Basaltic Rock Formations: Challenges for Optimizing Mineral-Fluid Reactions. *Pure Appl. Chem.* **2017**, *89* (5), 581−596.
(34) Schaef, H. T.; McGrail, B. P.; Owen, A. T. Carbonate Mineralization of Volcanic Province Basalts. *Int. J. Greenhouse Gas Control* **2010**, *4* (2), 249−261.
(35) Goldberg, D. S.; Takahashi, T.; Slagle, A. L. Carbon Dioxide Sequestration in Deep-Sea Basalt. *Proc. Natl. Acad. Sci. U. S. A.* **2008**, *105* (29), 9920−9925.
(36) Zevenhoven, R.; Fagerlund, J.; Songok, J. K. CO2 mineral Sequestration: Developments toward Large-scale Application. *Greenhouse Gases: Sci. Technol.* **2011**, *1* (1), 48−57.
(37) Intergovernmental Panel on Climate Change. *IPCC Special Report on Carbon Dioxide Capture and Storage*, Cambridge Univ. Press, 2005.
(38) Geerlings, H.; Zevenhoven, R. CO2 mineralization—Bridge Between Storage and Utilization of CO2. *Annu. Rev. Chem. Biomol. Eng.* **2013**, *4* (1), 103−117.
(39) Bonto, M.; Welch, M. J.; Lüthje, M.; Andersen, S. I.; Veshareh, M. J.; Amour, F.; Afrough, A.; Mokhtari, R.; Hajiabadi, M. R.; Alizadeh, M. R.; Larsen, C. N.; Nick, H. M. Challenges and Enablers for Large-Scale CO2 Storage in Chalk Formations. *Earth-Sci. Rev.* **2021**, *222* (September), No. 103826.
(40) Raza, A.; Glatz, G.; Gholami, R.; Mahmoud, M.; Alafnan, S. Carbon Mineralization and Geological Storage of CO2 in Basalt: Mechanisms and Technical Challenges. *Earth-Sci. Rev.* **2022**, *229* (March), No. 104036.
(41) Eyinla, D. S.; Leggett, S.; Badrouchi, F.; Emadi, H.; Adamolekun, O. J.; Akinsanpe, O. T. A Comprehensive Review of the Potential of Rock Properties Alteration during CO2 Injection for EOR and Storage. *Fuel* **2023**, *353* (June), No. 129219.
(42) Kim, K.; Kim, D.; Na, Y.; Song, Y.; Wang, J. A Review of Carbon Mineralization Mechanism during Geological CO2 Storage. *Heliyon* **2023**, *9* (12), No. e23135.
(43) Lu, P.; Apps, J.; Zhang, G.; Gysi, A.; Zhu, C. Knowledge Gaps and Research Needs for Modeling CO2 mineralization in the Basalt-CO2-Water System: A Review of Laboratory Experiments. *Earth-Sci. Rev.* **2024**, *254*, No. 104813.
(44) Bashir, A.; Ali, M.; Patil, S.; Aljawad, M. S.; Mahmoud, M.; Al-Shehri, D.; Hoteit, H.; Kamal, M. S. Comprehensive Review of CO2 Geological Storage: Exploring Principles, Mechanisms, and Prospects. *Earth-Sci. Rev.* **2024**, *249* (December 2023), No. 104672.
(45) Abdel Aal, A. Y. Mineral and Chemical Composition of Basalts in the Neighbourhood of Giza, Egypt. *J. Afr. Earth Sci.* **1998**, *26* (1), 101−117.
(46) Gislason, S. R.; Wolff-Boenisch, D.; Stefansson, A.; Oelkers, E. H.; Gunnlaugsson, E.; Sigurdardottir, H.; Sigfusson, B.; Broecker, W. S.; Matter, J. M.; Stute, M. Mineral Sequestration of Carbon Dioxide in Basalt: A Pre-Injection Overview of the CarbFix Project. *Int. J. Greenhouse Gas Control* **2010**, *4* (3), 537−545.
(47) The Groundwater Project. Hydrogeologic Properties of Earth Materials and Principles of Groundwater Flow. https://books.gw-project.org/hydrogeologic-properties-of-earth-materials-and-principles-of-groundwater-flow/chapter/effective-porosity/ (accessed 2024−06−06).
(48) Fisher, A. T. Permeability within Basaltic Oceanic Crust. *Rev. Geophys.* **1998**, *36* (2), 143−182.
(49) Gray, K. *Carbon Storage Atlas (Fifth Edition)* Office of Scientific and Technical Information (OSTI): Pittsburgh, PA, and Morgantown, WV (United States); 2015, DOI: 10.2172/1814017.
(50) Krajick, K. Scientists Target East Coast Rocks For CO2 Storage. State of the Planet. https://news.climate.columbia.edu/2010/01/04/scientists-target-east-coast-rocks-for-co2-storage/ (accessed 2024−04−11).
(51) Stanfield, C. H.; Miller, Q. R. S.; Battu, A. K.; Lahiri, N.; Nagurney, A. B.; Cao, R.; Nienhuis, E. T.; DePaolo, D. J.; Latta, D. E.; Schaef, H. T. Carbon Mineralization and Critical Mineral Resource Evaluation Pathways for Mafic−Ultramafic Assets. *ACS Earth Space Chem.* **2024**, *8* (6), 1204−1213.

(52) Cao, R.; Miller, Q.; Davidson, C.; Gallin, W.; Reidel, S.; Jiao, Z.; McLaughlin, F.; Schaef, H. Gigaton Commercial-Scale Carbon Storage and Mineralization Potential in Stacked Columbia River Basalt Reservoirs. October 27, 2023. DOI: 10.21203/rs.3.rs-2679618/v1.
(53) Sigfusson, B.; Gislason, S. R.; Matter, J. M.; Stute, M.; Wolff-boenisch, D.; Arnarsson, M. T.; Oelkers, E. H.; et al. Solving the Carbon-Dioxide Buoyancy Challenge: The Design and Field Testing of a Dissolved CO2 Injection System. *Int. J. Greenhouse Gas Control* **2015**, *37*, 213−219.
(54) Alzayani, A.; AlYousef, Z.; Almajid, M. M. CO2 Geological Sequestration in Basalt Formations. JPT. https://jpt.spe.org/twa/co2-geological-sequestration-in-basalt-formations (accessed 2023−05−12).
(55) Matter, J.; Stute, M.; Oelkers, E. H. Rapid Carbon Mineralization for Permanent Disposal of Anthropogenic Carbon Dioxide Emissions. *Science* **2016**, *352* (6291), 1312−1314, DOI: 10.1126/science.aad8132.
(56) International Energy Agency. *CO2 Storage Resources and Their Development: An IEA CCUS Handbook*; International Energy Agency DOI: 10.1787/9f492c0b-en.
(57) Snæbjörnsdóttir, S.; Oelkers, E. H.; Mesfin, K.; Aradóttir, E. S.; Dideriksen, K.; Gunnarsson, I.; Gunnlaugsson, E.; Matter, J. M.; Stute, M.; Gislason, S. R. The Chemistry and Saturation States of Subsurface Fluids during the in Situ Mineralisation of CO2 and H2S at the CarbFix Site in SW-Iceland. *Int. J. Greenhouse Gas Control* **2017**, *58*, 87−102.
(58) Druckenmiller, M. L.; Maroto-Valer, M. M.; Hill, M. Investigation of Carbon Sequestration via Induced Calcite Formation in Natural Gas Well Brine. *Energy Fuels* **2006**, *20* (1), 172−179.
(59) Steel, L.; Liu, Q.; Mackay, E.; Maroto-valer, M. M. Review CO2 Solubility Measurements in Brine under Reservoir Conditions: A Comparison of Experimental and Geochemical Modeling Methods. 2016, *217*, 197−217. DOI: 10.1002/ghg.
(60) Adamczyk, K.; Prémont-Schwarz, M.; Pines, D.; Pines, E.; Nibbering, E. T. J. Real-Time Observation of Carbonic Acid Formation in Aqueous Solution. *Science* **2009**, *326* (5960), 1690−1694.
(61) Hills, C. D.; Tripathi, N.; Carey, P. J. Mineralization Technology for Carbon Capture, Utilization, and Storage. *Front. Energy Res.* **2020**, *8* (July), 142.
(62) Snæbjörnsdóttir, S. Ó.; Gislason, S. R. CO2 Storage Potential of Basaltic Rocks Offshore Iceland. *Energy Procedia* **2016**, *86* (February), 371−380.
(63) Oelkers, E. H.; Gislason, S. R.; Matter, J. Mineral Carbonation of CO2. *Elements* **2008**, *4* (5), 333−337.
(64) Gislason, S. R.; Oelkers, E. H. Mechanism, Rates, and Consequences of Basaltic Glass Dissolution: II. An Experimental Study of the Dissolution Rates of Basaltic Glass as a Function of PH and Temperature. *Geochim. Cosmochim. Acta* **2003**, *67* (20), 3817−3832.
(65) Schaef, H. T.; McGrail, B. P.; Owen, A. T. Basalt-CO2−H2O Interactions and Variability in Carbonate Mineralization Rates. *Energy Procedia* **2009**, *1* (1), 4899−4906.
(66) Rosenbauer, R. J.; Thomas, B.; Bischoff, J. L.; Palandri, J. Carbon Sequestration via Reaction with Basaltic Rocks: Geochemical Modeling and Experimental Results. *Geochim. Cosmochim. Acta* **2012**, *89*, 116−133.
(67) Delerce, S.; Bénézeth, P.; Schott, J.; Oelkers, E. H. The Dissolution Rates of Naturally Altered Basalts at PH 3 and 120 °C: Implications for the in-Situ Mineralization of CO2 Injected into the Subsurface. *Chem. Geol.* **2023**, *621* (December 2022), No. 121353.
(68) Cao, X.; Li, Q.; Xu, L.; Tan, Y. A Review of in Situ Carbon Mineralization in Basalt. *J. Rock Mech. Geotech. Eng.* **2024**, *16* (4), 1467−1485.
(69) Knauss, K. G.; Nguyen, S. N.; Weed, H. C. Diopside Dissolution Kinetics as a Function of PH, CO2, Temperature, and Time. *Geochim. Cosmochim. Acta* **1993**, *57* (2), 285−294.
(70) Gudbrandsson, S.; Wolff-boenisch, D.; Gislason, S. R.; Oelkers, E. H. An Experimental Study of Crystalline Basalt Dissolution from 2 ⩽ PH ⩽ 11 and Temperatures from 5 to 75° C. *Geochim. Cosmochim. Acta* **2011**, *75* (19), 5496−5509.
(71) Pokrovsky, O. S.; Schott, J. Kinetics and Mechanism of Forsterite Dissolution at 25°C and PH from 1 to 12. *Geochim. Cosmochim. Acta* **2000**, *64* (19), 3313−3325.
(72) Schott, J.; Pokrovsky, O. S.; Oelkers, E. H. The Link Between Mineral Dissolution/Precipitation Kinetics and Solution Chemistry. *Rev. Mineral. Geochem.* **2009**, *70* (1), 207−258.
(73) Heřmanská, M.; Voigt, M. J.; Marieni, C.; Declercq, J.; Oelkers, E. H. A Comprehensive and Consistent Mineral Dissolution Rate Database: Part II: Secondary Silicate Minerals. *Chem. Geol.* **2023**, *636* (March), No. 121632.
(74) Pollyea, R. M.; Rimstidt, J. D. Rate Equations for Modeling Carbon Dioxide Sequestration in Basalt. *Appl. Geochem.* **2017**, *81*, 53−62.
(75) Eick, M. J.; Grossl, P. R.; Golden, D. C.; Sparks, D. L.; Ming, D. W. Dissolution of a Lunar Basalt Simulant as Affected by PH and Organic Anions. *Geoderma* **1996**, *74* (1−2), 139−160.
(76) Hänchen, M.; Prigiobbe, V.; Storti, G.; Seward, T. M.; Mazzotti, M. Dissolution Kinetics of Fosteritic Olivine at 90−150°C Including Effects of the Presence of CO2. *Geochim. Cosmochim. Acta* **2006**, *70* (17), 4403−4416.
(77) Berger, G.; Claparols, C.; Guy, C.; Daux, V. Dissolution Rate of a Basalt Glass in Silica-Rich Solutions: Implications for Long-Term Alteration. *Geochim. Cosmochim. Acta* **1994**, *58* (22), 4875−4886.
(78) Dou, W.; Geng, C.; Lin, M.; Jiang, W.; Ji, L.; Cao, G. A Pore-Scale Phase Field Model for CO2 − Fluid−Basalt Interactions. *ACS Omega* **2024**, *9* (26), 28648−28658.
(79) Wang, F.; Giammar, D. E. Forsterite Dissolution in Saline Water at Elevated Temperature and High CO2 Pressure. *Environ. Sci. Technol.* **2013**, *47* (1), 168−173.
(80) Prigiobbe, V.; Costa, G.; Baciocchi, R.; Hänchen, M.; Mazzotti, M. The Effect of CO2 and Salinity on Olivine Dissolution Kinetics at 120C. *Chem. Eng. Sci.* **2009**, *64* (15), 3510−3515.
(81) Stillings, L. L.; Brantley, S. L. Feldspar Dissolution at 25°C and PH 3: Reaction Stoichiometry and the Effect of Cations. *Geochim. Cosmochim. Acta* **1995**, *59* (8), 1483−1496.
(82) Clark, D. E.; Oelkers, E. H.; Gunnarsson, I.; Sigfússon, B.; Snæbjörnsdóttir, S.; Aradóttir, E. S.; Gíslason, S. R. CarbFix2: CO2 and H2S Mineralization during 3.5 years of Continuous Injection into Basaltic Rocks at More than 250 °C. *Geochim. Cosmochim. Acta* **2020**, *279*, 45−66.
(83) Flaathen, T. K.; Gislason, S. R.; Oelkers, E. H. The Effect of Aqueous Sulphate on Basaltic Glass Dissolution Rates. *Chem. Geol.* **2010**, *277* (3−4), 345−354.
(84) Min, Y.; Kubicki, J. D.; Jun, Y.-S. Plagioclase Dissolution during CO2 − SO 2 Cosequestration: Effects of Sulfate. *Environ. Sci. Technol.* **2015**, *49* (3), 1946−1954.
(85) van Noort, R.; Spiers, C. J.; Drury, M. R.; Kandianis, M. T. Peridotite Dissolution and Carbonation Rates at Fracture Surfaces under Conditions Relevant for in Situ Mineralization of CO2. *Geochim. Cosmochim. Acta* **2013**, *106*, 1−24.
(86) Wang, J.; Yagi, M.; Tamagawa, T.; Hirano, H.; Watanabe, N. Reactivity and Dissolution Characteristics of Naturally Altered Basalt in CO2 -Rich Brine: Implications for CO2 mineralization. *ACS Omega* **2024**, *9* (4), 4429−4438.
(87) Sun, C.; Yao, Z.; Wang, Q.; Guo, L.; Shen, X. Theoretical Study on the Organic Acid Promoted Dissolution Mechanism of Forsterite Mineral. *Appl. Surf. Sci.* **2023**, *614*, No. 156063, DOI: 10.1016/j.apsusc.2022.156063.
(88) Franklin, S. P.; Hajash, A.; Dewers, T. A.; Tieh, T. T. The Role of Carboxylic Acids in Albite and Quartz Dissolution: An Experimental Study under Diagenetic Conditions. *Geochim. Cosmochim. Acta* **1994**, *58* (20), 4259−4279.
(89) Guy, C.; Schott, J. Multisite Surface Reaction versus Transport Control during the Hydrolysis of a Complex Oxide. *Chem. Geol.* **1989**, *78* (3−4), 181−204.
(90) Wolff-Boenisch, D.; Wenau, S.; Gislason, S. R.; Oelkers, E. H. Dissolution of Basalts and Peridotite in Seawater, in the Presence of Ligands, and CO2: Implications for Mineral Sequestration of Carbon Dioxide. *Geochim. Cosmochim. Acta* **2011**, *75* (19), 5510−5525.

(91) Harouiya, N.; Oelkers, E. H. An Experimental Study of the Effect of Aqueous Fluoride on Quartz and Alkali-Feldspar Dissolution Rates. *Chem. Geol.* **2004**, *205* (1−2), 155−167.
(92) Matter, J. M.; Broecker, W. S.; Stute, M.; Gislason, S. R.; Oelkers, E. H.; Stefánsson, A. Permanent Carbon Dioxide Storage into Basalt: The CarbFix Pilot Project, Iceland. *Energy Procedia* **2009**, *1* (1), 3641−3646.
(93) Clark, D. E.; Gunnarsson, I.; Aradóttir, E. S.; Arnarson, M. P.; Porgeirsson, P. A.; Sigurardóttir, S. S.; Sigfússon, B.; Snæbjörnsdóttir, S.; Oelkers, E. H.; Gíslason, S. R. The Chemistry and Potential Reactivity of the CO2-H2S Charged Injected Waters at the Basaltic CarbFix2 Site, Iceland. In *Energy Procedia*; Elsevier B.V., 2018; Vol. *146*, pp 121−128 DOI: 10.1016/j.egypro.2018.07.016.
(94) Kanakiya, S.; Adam, L.; Esteban, L.; Rowe, M. C.; Shane, P. Dissolution and Secondary Mineral Precipitation in Basalts Due to Reactions with Carbonic Acid. *J. Geophys. Res.: Solid Earth* **2017**, *122* (6), 4312−4327, DOI: 10.1002/2017JB014019.
(95) Xiong, W.; Wells, R. K.; Horner, J. A.; Schaef, H. T.; Skemer, P. A.; Giammar, D. E. CO2 mineral Sequestration in Naturally Porous Basalt. *Environ. Sci. Technol. Lett.* **2018**, *5* (3), 142−147.
(96) Voigt, M.; Marieni, C.; Baldermann, A.; Galeczka, I. M.; Wolff-Boenisch, D.; Oelkers, E. H.; Gislason, S. R. An Experimental Study of Basalt−Seawater−CO2 Interaction at 130 °C. *Geochim. Cosmochim. Acta* **2021**, *308*, 21−41.
(97) Wolff-Boenisch, D. On the Buffer Capacity of CO2 -Charged Seawater Used for Carbonation and Subsequent Mineral Sequestration. *Energy Procedia* **2011**, *4* (December 2011), 3738−3745.
(98) Wolff-Boenisch, D.; Galeczka, I. M. Flow-through Reactor Experiments on Basalt-(Sea)Water-CO2 Reactions at 90 °C and Neutral PH. What Happens to the Basalt Pore Space under Post-Injection Conditions? *Int. J. Greenhouse Gas Control* **2018**, *68*, 176−190.
(99) Rigopoulos, I.; Harrison, A. L.; Delimitis, A.; Ioannou, I.; Efstathiou, A. M.; Kyratsi, T.; Oelkers, E. H. Carbon Sequestration via Enhanced Weathering of Peridotites and Basalts in Seawater. *Appl. Geochem.* **2018**, *91* (November 2017), 197−207.
(100) Luhmann, A. J.; Tutolo, B. M.; Tan, C.; Moskowitz, B. M.; Saar, M. O.; Seyfried, W. E. Whole Rock Basalt Alteration from CO2 -Rich Brine during Fl Ow-through Experiments at 150° C and 150 bar. *Chem. Geol.* **2017**, *453*, 92−110.
(101) Pajdak, A.; Skiba, M.; Gajda, A.; Anioł, Ł.; Kozieł, K.; Liu, J.; Berent, K.; Kudasik, M. Evolution of the Pore Structure as a Result of Mineral Carbonation of Basalts from Poland in the Context of Accumulation and Permanent Storage of CO2. *Int. J. Greenhouse Gas Control* **2024**, *137* (July), No. 104221.
(102) Kato, A.; Sakaguchi, A.; Yoshida, S.; Mochizuki, H.Permeability Measurements and Precipitation Sealing of Basalt in an Ancient Exhumed Subduction-Zone Fault *Bull. Earthq. Res. Inst.* 2003; Vol. *12*, pp 83−89 https://www2.jpgu.org/meeting/2003/pdf/j036/j036-004_e.pdf.
(103) Andreani, M.; Luquot, L.; Gouze, P.; Godard, M.; Hoisé, E.; Gibert, B. Experimental Study of Carbon Sequestration Reactions Controlled by the Percolation of CO2 -Rich Brine through Peridotites. *Environ. Sci. Technol.* **2009**, *43* (4), 1226−1231.
(104) Peuble, S.; Godard, M.; Gouze, P.; Leprovost, R.; Martinez, I.; Shilobreeva, S. Control of CO2 on Flow and Reaction Paths in Olivine-Dominated Basements: An Experimental Study. *Geochim. Cosmochim. Acta* **2019**, *252*, 16−38.
(105) Béarat, H.; McKelvy, M. J.; Chizmeshya, A. V. G.; Gormley, D.; Nunez, R.; Carpenter, R. W.; Squires, K.; Wolf, G. H. Carbon Sequestration via Aqueous Olivine Mineral Carbonation: Role of Passivating Layer Formation. *Environ. Sci. Technol.* **2006**, *40* (15), 4802−4808.
(106) Godard, M.; Luquot, L.; Andreani, M.; Gouze, P. Incipient Hydration of Mantle Lithosphere at Ridges: A Reactive-Percolation Experiment. *Earth Planet. Sci. Lett.* **2013**, *371*−*372*, 92−102.
(107) Hövelmann, J.; Austrheim, H.; Jamtveit, B. Microstructure and Porosity Evolution during Experimental Carbonation of a Natural Peridotite. *Chem. Geol.* **2012**, *334*, 254−265.
(108) Stavropoulou, E.; Griner, C.; Laloui, L. Impact of CO2-Rich Seawater Injection on the Flow Properties of Basalts. *Int. J. Greenhouse Gas Control* **2024**, *134* (October 2023), No. 104128.
(109) Guha Roy, D.; Vishal, V.; Singh, T. N. Effect of Carbon Dioxide Sequestration on the Mechanical Properties of Deccan Basalt. *Environ. Earth Sci.* **2016**, *75* (9), No. 771.
(110) Hellevang, H.; Haile, B. G.; Tetteh, A. Experimental Study to Better Understand Factors Affecting the CO2 mineral Trapping Potential of Basalt. *Greenhouse Gases: Sci. Technol.* **2017**, *7* (1), 143−157.
(111) Clark, D. E.; Galeczka, I. M.; Dideriksen, K.; Voigt, M. J.; Wolff-Boenisch, D.; Gislason, S. R. Experimental Observations of CO2-Water-Basaltic Glass Interaction in a Large Column Reactor Experiment at 50 °C. *Int. J. Greenhouse Gas Control* **2019**, *89* (January), 9−19.
(112) Gysi, A. P.; Stefánsson, A. CO2-Water−Basalt Interaction. Low Temperature Experiments and Implications for CO2 Sequestration into Basalts. *Geochim. Cosmochim. Acta* **2012**, *81*, 129−152.
(113) Giammar, D. E.; Bruant, R. G.; Peters, C. A. Forsterite Dissolution and Magnesite Precipitation at Conditions Relevant for Deep Saline Aquifer Storage and Sequestration of Carbon Dioxide. *Chem. Geol.* **2005**, *217* (3−4), 257−276.
(114) Wu, H.; Jayne, R. S.; Bodnar, R. J.; Pollyea, R. M. Simulation of CO2 mineral Trapping and Permeability Alteration in Fractured Basalt: Implications for Geologic Carbon Sequestration in Mafic Reservoirs. *Int. J. Greenhouse Gas Control* **2021**, *109* (February), No. 103383.
(115) Erol, S.; Akın, T.; Başer, A.; Saraçoğlu, Ö.; Akın, S. Fluid-CO2 Injection Impact in a Geothermal Reservoir: Evaluation with 3-D Reactive Transport Modeling. *Geothermics* **2022**, *98* (October 2021), No. 102271, DOI: 10.1016/j.geothermics.2021.102271.
(116) Al Maqbali, Q.; Hussain, S.; Mask, G.; Xingru, W. Numerical Simulation of In-Situ CO2 mineralization in Mafic Basaltic Formations in Southwest Oklahoma. In *Society of Petroleum Engineers - SPE Oklahoma City Oil and Gas Symposium 2023*; OKOG, 2023 DOI: 10.2118/213084-MS.
(117) Menefee, A. H.; Li, P.; Giammar, D. E.; Ellis, B. R. Roles of Transport Limitations and Mineral Heterogeneity in Carbonation of Fractured Basalts. *Environ. Sci. Technol.* **2017**, *51* (16), 9352−9362.
(118) Zhao, R.; Zhong, Z.; Yu, Y.; Lü, R.; Shi, T.; Wang, N.; Cheng, J. Numerical Simulation of CO2 Storage by Basalts in Xingouzui Formation, Jianghan Basin, China. *Int. J. Greenhouse Gas Control* **2024**, *134* (April), No. 104133.
(119) Khan, M. I.; Khanal, A. Machine Learning Assisted Prediction of Porosity and Related Properties Using Digital Rock Images. *ACS Omega* **2024**, *9*, 30205.
(120) Tariq, Z.; Ali, M.; Yan, B.; Sun, S.; Hoteit, H. Machine Learning Modeling of Saudi Arabian Basalt/CO2/Brine Wettability Prediction: Implications for CO2 Geo-Storage. In *57th U.S. Rock Mechanics/Geomechanics Symposium*; ARMA, 2023 DOI: 10.56952/ARMA-2023-0755.
(121) Song, Y.; Sung, W.; Jang, Y.; Jung, W. Application of an Artificial Neural Network in Predicting the Effectiveness of Trapping Mechanisms on CO2 Sequestration in Saline Aquifers. *Int. J. Greenhouse Gas Control* **2020**, *98* (April), No. 103042.
(122) Alfredsson, H. A.; Oelkers, E. H.; Hardarsson, B. S.; Franzson, H.; Gunnlaugsson, E.; Gislason, S. R. The Geology and Water Chemistry of the Hellisheidi, SW-Iceland Carbon Storage Site. *Int. J. Greenhouse Gas Control* **2013**, *12*, 399−418.
(123) Gislason, S. R.; Oelkers, E. H. Carbon Storage in Basalt. *Science* **2014**, *344* (6182), 373−374.
(124) Trias, R.; Ménez, B.; Le Campion, P.; Zivanovic, Y.; Lecourt, L.; Lecoeuvre, A.; Schmitt-Kopplin, P.; Uhl, J.; Gislason, S. R.; Alfreosson, H. A.; Mesfin, K. G.; Snæbjörnsdóttir, S. O.; Aradóttir, E. S.; Gunnarsson, I.; Matter, J. M.; Stute, M.; Oelkers, E. H.; Gérard, E. High Reactivity of Deep Biota under Anthropogenic CO2 Injection into Basalt. *Nat. Commun.* **2017**, *8* (1), No. 1063, DOI: 10.1038/s41467-017-01288-8.
(125) Gíslason, S. R.; Sigurdardóttir, H.; Aradóttir, E. S.; Oelkers, E. H. A Brief History of CarbFix: Challenges and Victories of the Project's Pilot Phase. *Energy Procedia* **2018**, *146*, 103−114.

(126) Sigfússon, B.; Arnarson, M. P.; Snæbjörnsdóttir, S. Ó.; Karlsdóttir, M. R.; Aradóttir, E. S.; Gunnarsson, I. Reducing Emissions of Carbon Dioxide and Hydrogen Sulphide at Hellisheidi Power Plant in 2014−2017 and the Role of CarbFix in Achieving the 2040 Iceland Climate Goals. *Energy Procedia* **2018**, *146*, 135−145.
(127) McGrail, B. P.; Schaef, H. T.; Spane, F. A.; Horner, J. A.; Owen, A. T.; Cliff, J. B.; Qafoku, O.; Thompson, C. J.; Sullivan, E. C. Wallula Basalt Pilot Demonstration Project: Post-Injection Results and Conclusions. In *Energy Procedia*; Elsevier B.V., 2017; Vol. *114*, pp 5783−5790 DOI: 10.1016/j.egypro.2017.03.1716.
(128) U.S. Department of Energy National Energy Technology Laboratory. Wallula Basalt Pilot Project. https://netl.doe.gov/coal/carbon-storage/atlas/bscsp/phase-II/wallula (accessed 2024−07−05).
(129) Snæbjörnsdóttir, S. Ó.; Sigfússon, B.; Marieni, C.; Goldberg, D.; Gislason, S. R.; Oelkers, E. H. Carbon Dioxide Storage through Mineral Carbonation. *Nat. Rev. Earth Environ.* **2020**, *1* (2), 90−102.
(130) McGrail, B. P.; Spane, F. A.; Amonette, J. E.; Thompson, C. R.; Brown, C. F. Injection and Monitoring at the Wallula Basalt Pilot Project. In *Energy Procedia*; Elsevier B.V., 2014; Vol. *63*, pp 2939−2948 DOI: 10.1016/j.egypro.2014.11.316.
(131) White, S. K.; Spane, F. A.; Schaef, H. T.; Miller, Q. R. S.; White, M. D.; Horner, J. A.; McGrail, B. P. Quantification of CO2Mineralization at the Wallula Basalt Pilot Project. *Environ. Sci. Technol.* **2020**, *54* (22), 14609−14616.
(132) Global CCS Institute. China Continues to Advance CCUS in 2023: "Learning-by-doing" after Launch of First Integrated Megaton Project Underscores Momentum. https://www.globalccsinstitute.com/news-media/insights/china-continues-to-advance-ccus-in-2023-learning-by-doing-after-launch-of-first-integrated-megaton-project-underscore-momentum/ (accessed 2023−05−12).
(133) GEOMAR. PERBAS: In search of safe carbon dioxide storage in offshore basalt rocks. https://www.geomar.de/en/news/article/perbas-in-search-of-safe-carbon-dioxide-storage-in-offshore-basalt-rocks (accessed 2024−05−11).
(134) Global CCS Institute. The Global Status of CCS. Global CCS Institute. http://www.globalccsinstitute.com/sites/default/files/global-status-css-final.pdf (accessed 2024−06−06).
(135) Seyyedi, M.; Mahmud, H. K. B.; Verrall, M.; Giwelli, A.; Esteban, L.; Ghasemiziarani, M.; Clennell, B. Pore Structure Changes Occur During CO2 Injection into Carbonate Reservoirs. *Sci. Rep.* **2020**, *10* (1), No. 3624.
(136) Khather, M.; Saeedi, A.; Myers, M. B.; Verrall, M. An Experimental Study for Carbonate Reservoirs on the Impact of CO2 -EOR on Petrophysics and Oil Recovery. *Fuel* **2019**, *235* (August 2018), 1019−1038.
(137) Akbar, M.; Vissapragada, B.; Alghamdi, A. H.; Allen, D.; Herron, M.; Carnegie, A.; Dutta, D.; Chourasiya, R. D.; Logan, D.; Stief, D.; Netherwood, R.; Russell, S. D.; Saxena, K. A Snapshot of Carbonate Reservoir Evaluation. *Oilfield Rev.* **1995**, *12* (4), 20−41.
(138) Salem, A. M.; Shedid, A. S. Variation of Petrophysical Properties Due to Carbon Dioxide (CO2) Storage in Carbonate Reservoirs. *J. Pet. Gas* **2013**, *4* (4), 91−102.
(139) Asghari, K.; Al-Dliwe, A. Optimization of Carbon Dioxide Sequestration and Improved Oil Recovery in Oil Reservoirs. *Greenh. Gas Control Technol.* **2005**, *I*, 381−389.
(140) Mazzullo, S. J. Overview of Porosity Evolution in Carbonate Reservoirs. *Kansas Geol. Soc. Bull.* **2004**, *79* (1-2), 1−19.
(141) Khather, M.; Saeedi, A.; Rezaee, R.; Noble, R. R. P.; Gray, D. Experimental Investigation of Changes in Petrophysical Properties during CO2 Injection into Dolomite-Rich Rocks. *Int. J. Greenhouse Gas Control* **2017**, *59*, 74−90.
(142) Warren, J. Dolomite: Occurrence, Evolution and Economically Important Associations. *Earth-Sci. Rev.* **2000**, *52* (1−3), 1−81.
(143) Berrezueta, E.; Kovacs, T.; Herrera-Franco, G.; Mora-Frank, C.; Caicedo-Potosí, J.; Carrion-Mero, P.; Carneiro, J. Laboratory Studies on CO2-Brine-Rock Interaction: An Analysis of Research Trends and Current Knowledge. *Int. J. Greenhouse Gas Control* **2023**, *123* (January), No. 103842.
(144) Jun, Y. S.; Giammar, D. E.; Werth, C. J. Impacts of Geochemical Reactions on Geologic Carbon Sequestration. *Environ. Sci. Technol.* **2013**, *47* (1), 3−8.
(145) Svensson, U.; Dreybrodt, W. Dissolution Kinetics of Natural Calcite Minerals in CO2-Water Systems Approaching Calcite Equilibrium. *Chem. Geol.* **1992**, *100* (1−2), 129−145.
(146) Luquot, L.; Gouze, P. Experimental Determination of Porosity and Permeability Changes Induced by Injection of CO2 into Carbonate Rocks. *Chem. Geol.* **2009**, *265* (1−2), 148−159.
(147) Mohamed, I. M.; He, J.; Mahmoud, M. A.; Nasr-El-Din, H. A. Effects of Pressure, CO2 Vol., and the CO2 to Water Vol.tric Ratio on Permeability Change During CO2 Sequestration. In *All Days*; SPE, 2010. DOI: 10.2118/136394-MS.
(148) Wang, J.; Zhao, Y.; An, Z.; Shabani, A. CO2 Storage in Carbonate Rocks: An Experimental and Geochemical Modeling Study. *J. Geochem. Explor.* **2022**, *234* (December 2021), No. 106942.
(149) Smith, M. M.; Hao, Y.; Carroll, S. A. Development and Calibration of a Reactive Transport Model for Carbonate Reservoir Porosity and Permeability Changes Based on CO2 Core-Flood Experiments. *Int. J. Greenhouse Gas Control* **2017**, *57*, 73−88.
(150) Segura, D.; Cerepi, A.; Loisy, C. Aquifer-CO2 Leak Project. Effect of CO2-Rich Water Percolation in Porous Limestone Cores: Simulation of a Leakage in a Shallow Carbonate Freshwater Aquifer. *Chem. Geol.* **2024**, *657*, No. 122105.
(151) Pokrovsky, O. S.; Golubev, S. V.; Schott, J.; Castillo, A. Calcite, Dolomite and Magnesite Dissolution Kinetics in Aqueous Solutions at Acid to Circumneutral PH, 25 to 150 °C and 1 to 55 Atm PCO2: New Constraints on CO2 Sequestration in Sedimentary Basins. *Chem. Geol.* **2009**, *265* (1−2), 20−32.
(152) Peng, C.; Crawshaw, J. P.; Maitland, G. C.; Trusler, J. P. M. Kinetics of Calcite Dissolution in CO2-Saturated Water at Temperatures between (323 and 373) K and Pressures up to 13.8 MPa. *Chem. Geol.* **2015**, *403*, 74−85.
(153) Menke, H. P.; Bijeljic, B.; Andrew, M. G.; Blunt, M. J. Dynamic Three-Dimensional Pore-Scale Imaging of Reaction in a Carbonate at Reservoir Conditions. *Environ. Sci. Technol.* **2015**, *49* (7), 4407−4414.
(154) Nomeli, M. A.; Riaz, A. Effect of CO2 Solubility on Dissolution Rate of Calcite in Saline Aquifers for Temperature Range of 50−100 °C and Pressures up to 600 bar: Alterations of Fractures Geometry in Carbonate Rocks by CO2-Acidified Brines. *Environ. Earth Sci.* **2017**, *76* (9), 352.
(155) Gledhill, D. K.; Morse, J. W. Calcite Dissolution Kinetics in Na−Ca−Mg−Cl Brines. *Geochim. Cosmochim. Acta* **2006**, *70* (23), 5802−5813.
(156) Tan, Y.; Li, Q.; Xu, L.; Onyekwena, C. C.; Yu, T.; Xu, L. Effects of SiO 2 Nanoparticles on Wettability and CO2 − Brine−Rock Interactions in Carbonate Reservoirs: Implications for CO2 Storage. *Energy Fuels* **2024**, *38* (2), 1258−1270.
(157) Haghtalab, A.; Mohammadi, M.; Fakhroueian, Z. Absorption and Solubility Measurement of CO2 in Water-Based ZnO and SiO2 Nanofluids. *Fluid Phase Equilib.* **2015**, *392*, 33−42.
(158) Isah, A.; Mahmoud, M.; Raza, A.; Murtaza, M.; Arif, M.; Kamal, M. S. CO2-Brine Interactions in Anhydrite-Rich Rock: Implications for Carbon Mineralization and Geo-Storage. *Int. J. Greenhouse Gas Control* **2024**, *137* (July), No. 104202.
(159) Karaei, M. A.; Honarvar, B.; Azdarpour, A.; Mohammadian, E. Co2 Storage in Low Permeable Carbonate Reservoirs: Permeability and Interfacial Tension (Ift) Changes during Co2 Injection in an Iranian Carbonate Reservoir. *Period. Polytech. Chem. Eng.* **2020**, *64* (4), 491−504.
(160) He, L.; Zhao, L.; Li, J.; Ma, J.; Lui, R.; Wang, S.; Zhao, W. Complex Relationship between Porosity and Permeability of Carbonate Reservoirs and Its Controlling Factors: A Case Study of Platform Facies in Pre-Caspian Basin. *Pet. Explor. Dev.* **2014**, *41* (2), 225−234.
(161) Oomole, O.; Osoba, J. S. Carbon Dioxide - Dolomite Rock Interaction During CO_2 Flooding Process. In *Annual Technical Meeting*; Petroleum Society of Canada, 1983 DOI: 10.2118/83-34-17.

(162) Rosenbauer, R. J.; Koksalan, T.; Palandri, J. L. Experimental Investigation of CO2−Brine−Rock Interactions at Elevated Temperature and Pressure: Implications for CO2 Sequestration in Deep-Saline Aquifers. *Fuel Process. Technol.* **2005**, *86* (14−15), 1581−1597.
(163) Cui, G.; Zhang, L.; Tan, C.; Ren, S.; Zhuang, Y.; Enechukwu, C. Injection of Supercritical CO2 for Geothermal Exploitation from Sandstone and Carbonate Reservoirs: CO2 − Water − Rock Interactions and Their e Ff Ects. *J. CO2 Util.* **2017**, *20* (May), 113−128.
(164) Detwiler, R. L. Experimental Observations of Deformation Caused by Mineral Dissolution in Variable-Aperture Fractures. *J. Geophys. Res.: Solid Earth* **2008**, *113* (8), 1−12.
(165) Luhmann, A. J.; Kong, X.; Tutolo, B. M.; Garapati, N.; Bagley, B. C.; Saar, M. O.; Seyfried, W. E., Jr Experimental Dissolution of Dolomite by CO2-Charged Brine at 100 °C and 150bar: Evolution of Porosity, Permeability, and Reactive Surface Area. *Chem. Geol.* **2014**, *380*, 145−160, DOI: 10.1016/j.chemgeo.2014.05.001.
(166) Ciantia, M. O.; Castellanza, R.; Crosta, G. B.; Hueckel, T. Effects of Mineral Suspension and Dissolution on Strength and Compressibility of Soft Carbonate Rocks. *Eng. Geol.* **2015**, *184*, 1−18.
(167) Liteanu, E.; Spiers, C. J.; de Bresser, J. H. P. The Influence of Water and Supercritical CO2 on the Failure Behavior of Chalk. *Tectonophysics* **2013**, *599*, 157−169.
(168) André, L.; Audigane, P.; Azaroual, M.; Menjoz, A. Numerical Modeling of Fluid-Rock Chemical Interactions at the Supercritical CO2-Liquid Interface during CO2 Injection into a Carbonate Reservoir, the Dogger Aquifer (Paris Basin, France). *Energy Convers. Manage.* **2007**, *48* (6), 1782−1797.
(169) Ben Mahmud, H.; Mahmud, W. M.; Al-Rubaye, A. Modeling Interaction between CO2, Brine and Chalk Reservoir Rock Including Temperature Effect on Petrophysical Properties. *Energy Geosci.* **2021**, *2* (4), 337−344.
(170) Al Salmi, H.; Kazemi, A.; Ganat, T. Unveiling the Effects of CO2 Injection on Reservoir Aquifer Properties. *Energy Fuels* **2024**, *38* (17), 16705−16712.
(171) Zhu, G.; Wei, Z.; Wu, X.; Li, Y. New Insights into the Dolomitization and Dissolution Mechanisms of Dolomite-Calcite (104)/(110) Crystal Boundary: An Implication to Geologic Carbon Sequestration Process. *Sci. Total Environ.* **2023**, *904*, No. 166273.
(172) Bello, A.; Dorhjie, D. B.; Ivanova, A.; Cheremisin, A. Numerical Sensitivity Analysis of CO2 mineralization Trapping Mechanisms in a Deep Saline Aquifer. *Chem. Eng. Sci.* **2024**, *283*, No. 119335.
(173) Li, P.; Hao, Y.; Wu, Y.; Wanniarachchi, A.; Zhang, H.; Cui, Z. Experimental Study on the Effect of CO2 Storage on the Reservoir Permeability in a CO2-Based Enhanced Geothermal System. *Geotherm. Energy* **2023**, *11* (1), No. 24.
(174) Cui, G.; Ren, S.; Zhang, L.; Wang, Y.; Zhang, P. Injection of Supercritical CO2 for Geothermal Exploitation from Single- and Dual-Continuum Reservoirs: Heat Mining Performance and Salt Precipitation Effect. *Geothermics* **2018**, *73* (November 2017), 48−59.
(175) Mouallem, J.; Arif, M.; Mahmoud, M. Numerical Simulation of CO2 mineral Trapping Potential of Carbonate Rocks. In *Day 2 Tue, March 14, 2023*; SPE, 2023 DOI: 10.2118/214162-MS.
(176) Kirmani, F. U. D.; Raza, A.; Ahmad, S.; Arif, M.; Mahmoud, M. A Holistic Overview of the In-Situ and Ex-Situ Carbon Mineralization: Methods, Mechanisms, and Technical Challenges. *Sci. Total Environ.* **2024**, *943* (January), No. 173836.
(177) Budinis, S.; Krevor, S.; Dowell, N. M.; Brandon, N.; Hawkes, A. An Assessment of CCS Costs, Barriers and Potential. *Energy Strategy Rev.* **2018**, *22* (May), 61−81.
(178) U.S. Department of Energy National Energy Technology Laboratory. FECM/NETL CO2 Capture, Transport and Storage (CTS) Cost Screening Tool. https://netl.doe.gov/energy-analysis/details?id=2c3a1880-3ed2-46a2-adad-8d11f767fa15 (accessed 2024−11−10).
(179) Guinan, A.; Sheriff, A.; Basista, E.; Shih, C.; Hoffman, H.; Grant, T.*Evaluating CCS Cost Options for CO_2 Sources in the Central United States*, Office of Scientific and Technical Information (OSTI), 2023, DOI: 10.2172/2202570.
(180) Moch, J. M.; Xue, W.; Holdren, J. P. Carbon Capture, Utilization, and Storage: Technologies and Costs in the U.S. Context. https://www.belfercenter.org/sites/default/files/pantheon_files/files/publication/Brief_CCUS_FINAL.pdf (accessed 2023−06−05).
(181) Hong, W. Y. A Techno-Economic Review on Carbon Capture, Utilisation and Storage Systems for Achieving a Net-Zero CO2 Emissions Future. *Carbon Capture Sci. Technol.* **2022**, *3*. 100044.
(182) Smith, K. H.; Ashkanani, H. E.; Morsi, B. I.; Siefert, N. S. Physical Solvents and Techno-Economic Analysis for Pre-Combustion CO2 Capture: A Review. *Int. J. Greenhouse Gas Control* **2022**, *118* (May), No. 103694.
(183) Energy, U. S. D. of. Pre-Combustion Carbon Capture Research. https://www.energy.gov/fecm/pre-combustion-carbon-capture-research# Today's commercially available pre-combustion,cycle (IGCC) power plant. (accessed 2024−12−08).
(184) Zanco, S. E.; Pérez-Calvo, J.-F.; Gasós, A.; Cordiano, B.; Becattini, V.; Mazzotti, M. Postcombustion CO2 Capture: A Comparative Techno-Economic Assessment of Three Technologies Using a Solvent, an Adsorbent, and a Membrane. *ACS Eng. Au* **2021**, *1* (1), 50−72.
(185) Rubin, E. S.; Davison, J. E.; Herzog, H. J. The Cost of CO2 Capture and Storage. *Int. J. Greenhouse Gas Control* **2015**, *40*, 378−400.
(186) Idem, R.; Supap, T.; Shi, H.; Gelowitz, D.; Ball, M.; Campbell, C.; Tontiwachwuthikul, P. Practical Experience in Post-Combustion CO2 Capture Using Reactive Solvents in Large Pilot and Demonstration Plants. *Int. J. Greenhouse Gas Control* **2015**, *40* (2015), 6−25.
(187) Fleiß, B.; Priscak, J.; Hammerschmid, M.; Fuchs, J.; Müller, S.; Hofbauer, H. CO2 Capture Costs of Chemical Looping Combustion of Biomass: A Comparison of Natural and Synthetic Oxygen Carrier. *J. Energy Chem.* **2024**, *92*, 296−310.
(188) Vega, F.; Camino, S.; Camino, J. A.; Garrido, J.; Navarrete, B. Partial Oxy-Combustion Technology for Energy Efficient CO2 Capture Process. *Appl. Energy* **2019**, *253*. 113519.
(189) Talei, S.; Fozer, D.; Varbanov, P. S.; Szanyi, A.; Mizsey, P. Oxyfuel Combustion Makes Carbon Capture More Efficient. *ACS Omega* **2024**, *9* (3), 3250−3561, DOI: 10.1021/acsomega.3c05034.
(190) Sabatino, F.; Grimm, A.; Gallucci, F.; van Sint Annaland, M.; Kramer, G. J.; Gazzani, M. A Comparative Energy and Costs Assessment and Optimization for Direct Air Capture Technologies. *Joule* **2021**, *5* (8), 2047−2076.
(191) Lackner, K. S.; Azarabadi, H. Buying down the Cost of Direct Air Capture. *Ind. Eng. Chem. Res.* **2021**, *60* (22), 8196−8208.
(192) International Energy Agency. CO2 Capture and Storage: A Key Abatement Option. In *Energy Technology Analysis*; OECD, 2008; pp 61−130 .
(193) Zhao, X.; Xiao, J.; Hou, J.; Wu, J.; Lyu, X.; Zhang, J.; Liu, Y. Economic and Scale Prediction of CO2 Capture, Utilization and Storage Technologies in China. *Pet. Explor. Dev.* **2023**, *50* (3), 657−668.
(194) Psarras, P.; He, J.; Pilorgé, H.; McQueen, N.; Jensen-Fellows, A.; Kian, K.; Wilcox, J. Cost Analysis of Carbon Capture and Sequestration from U.S. Natural Gas-Fired Power Plants. *Environ. Sci. Technol.* **2020**, *54* (10), 6272−6280.
(195) U.S. Department of Transportation. Annual Report Mileage for Hazardous Liquid or Carbon Dioxide Systems. https://www.phmsa.dot.gov/data-and-statistics/pipeline/annual-report-mileage-hazardous-liquid-or-carbon-dioxide-systems (accessed 2024−12−07).
(196) Intergovernmental Panel on Climate Change. IPCC Special Report on Carbon Dioxide Capture and Storage: Chapter 4 - Transport of CO2. Cambridge University Press. https://www.ipcc.ch/site/assets/uploads/2018/03/srccs_chapter4-1.pdf (accessed 2024−07−12).
(197) Smith, E.; Morris, J.; Kheshgi, H.; Teletzke, G.; Herzog, H.; Paltsev, S. The Cost of CO2 Transport and Storage in Global Integrated Assessment Modeling. *SSRN Electron. J.* **2021**, *109*, No. 103367, DOI: 10.2139/ssrn.3816593.
(198) Schmelz, W. J.; Hochman, G.; Miller, K. G. Total Cost of Carbon Capture and Storage Implemented at a Regional Scale:

Northeastern and Midwestern United States. *Interface Focus* **2020**, *10* (5), No. 20190065, DOI: 10.1098/rsfs.2019.0065.
(199) Kelemen, P.; Benson, S. M.; Pilorgé, H.; Psarras, P.; Wilcox, J. An Overview of the Status and Challenges of CO2 Storage in Minerals and Geological Formations. *Front. Clim.* **2019**, *1*, 9 DOI: 10.3389/fclim.2019.00009.
(200) U.S. Department of Energy. IRA and Carbon Management Opportunities in Western Tribal Nations. Office of Fossil energy and Carbon Management. https://www.energy.gov/sites/default/files/2023-05/IRAandCarbonManagementOpportunitiesinWesternTribalNations_May2023.pdf (accessed 2024−07−12).
(201) Global CCS Institute. Understanding Industrial CCS Hubs and Clusters. Global CCS Institute. https://www.globalccsinstitute.com/wp-content/uploads/2019/08/Understanding-Industrial-CCS-hubs-and-clusters.pdf (accessed 2024−06−06).
(202) Miri, R. Effects of CO2 -Brine-Rock Interactions on CO2 Injectivity − Implications for CCS, University of Oslo, 2015. https://www.duo.uio.no/bitstream/handle/10852/48598/PhD-Miri-DUO.pdf?sequence=1&isAllowed=y.
(203) Raza, A.; Rezaee, R.; Gholami, R.; Rasouli, V.; Bing, C. H.; Nagarajan, R.; Hamid, M. A. Injectivity and Quantification of Capillary Trapping for CO2 Storage: A Review of Influencing Parameters. *J. Nat. Gas Sci. Eng.* **2015**, *26*, 510−517.
(204) Watson, M. N.; Gibson-Poole, C. M. Reservoir Selection for Optimised Geological Injection and Storage of Carbon Dioxide: A Combined Geochemical and Stratigraphic Perspective. In *4th Annual Conference on Carbon Capture and Sequestration*, 2005.
(205) Bacci, G.; Korre, A.; Durucan, S. Experimental Investigation into Salt Precipitation during CO2 Injection in Saline Aquifers. *Energy Procedia* **2011**, *4*, 4450−4456.
(206) Bemer, E.; Lombard, J. M. From Injectivity to Integrity Studies of CO_2Geological Storage. *Oil Gas Sci. Technol.* **2010**, *65* (3), 445−459.
(207) Liu, D.; Agarwal, R.; Li, Y.; Yang, S. Reactive Transport Modeling of Mineral Carbonation in Unaltered and Altered Basalts during CO2 Sequestration. *Int. J. Greenhouse Gas Control* **2019**, *85* (November 2018), 109−120.
(208) Hosseini, S. A.; Alfi, M.; Nicot, J. P.; Nuñez-Lopez, V. Analysis of CO2 Storage Mechanisms at a CO2-EOR Site, Cranfield, Mississippi. *Greenhouse Gases: Sci. Technol.* **2018**, *8* (3), 469−482.
(209) Sedaghatinasab, R.; Kord, S.; Moghadasi, J.; Soleymanzadeh, A. Relative Permeability Hysteresis and Capillary Trapping during CO2 EOR and Sequestration. *Int. J. Greenhouse Gas Control* **2021**, *106*. 103262.
(210) Kaldi, J.; Daniel, R.; Tenthorey, E.; Michae, K.; Schacht, U.; Nicol, A.; Underschultz, J.; Backe, G. Containment of CO2 in CCS: Role of Caprocks and Faults. *Energy Procedia* **2013**, *37*, 5403−5410.
(211) Busch, A.; Amann, A.; Bertier, P.; Waschbusch, M.; Krooss, B. M.The Significance of Caprock Sealing Integrity for CO2 Storage. In *Society of Petroleum Engineers - SPE International Conference on CO2 Capture, Storage, and Utilization 2010*; SPE, 2010; pp 300−307 .
(212) Wollenweber, J.; Alles, S.; Busch, A.; Krooss, B. M.; Stanjek, H.; Littke, R. Experimental Investigation of the CO2 Sealing Efficiency of Caprocks. *Int. J. Greenhouse Gas Control* **2010**, *4* (2), 231−241.
(213) Busch, A.; Alles, S.; Gensterblum, Y.; Prinz, D.; Dewhurst, D. N.; Raven, M. D.; Stanjek, H.; Krooss, B. M. Carbon Dioxide Storage Potential of Shales. *Int. J. Greenhouse Gas Control* **2008**, *2* (3), 297−308.
(214) D'Aniello, A.; Tómasdóttir, S.; Sigfússon, B.; Fabbricino, M. Modeling Gaseous CO2 Flow Behavior in Layered Basalts: Dimensional Analysis and Aquifer Response. *Groundwater* **2021**, *59* (5), 677−693.
(215) IEAGHG. A Review of the In'tl State of the Art in Risk Assessment Guidelines and Proposed Termimology for Use in CO2 Geological Storage. https://ieaghg.org/publications/a-review-of-the-intl-state-of-the-art-in-risk-assessment-guidelines-and-proposed-termimology-for-use-in-co2-geological-storage/ (accessed 2024−07−12).
(216) Dean, M.; Blackford, J.; Connelly, D.; Hines, R. Insights and Guidance for Offshore CO2 Storage Monitoring Based on the QICS, ETI MMV, and STEMM-CCS Projects. *Int. J. Greenhouse Gas Control* **2020**, *100*, No. 103120.
(217) Tanaka, Y.; Sawada, Y.; Tanase, D.; Tanaka, J.; Shiomi, S.; Kasukawa, T. Tomakomai CCS Demonstration Project of Japan, CO2 Injection in Process. *Energy Procedia* **2017**, *114*, 5836−5846.
(218) Benson, S.; Akai, M.; Caldeira, K.; de Coninck, H.; Cook, P.; Davidson, O.; Doctor, R.; Dooley, J.; Freund, P.; Gale, J.; Heidug, W.; Herzog, H.; Keith, D.; Mazzotti, M.; Metz, B.; Meyer, L.; Osman-Elasha, B.; Palmer, A.; Pipatti, R.; Rubin, E.; Smekens, K.; Soltanieh, M.; Thambimuthu, K. Kailai. Carbon Dioxide Capture and Storage. *IPCC Special Report* **2005**, *58*, 297−348.
(219) Khatiwada, M.; Adam, L.; Morrison, M.; van Wijk, K. A Feasibility Study of Time-Lapse Seismic Monitoring of CO2 Sequestration in a Layered Basalt Reservoir. *J. Appl. Geophys.* **2012**, *82*, 145−152.
(220) Matter, J. M.; Stute, M.; Hall, J.; Mesfin, K.; Snæbjörnsdóttir, S.; Gislason, S. R.; Oelkers, E. H.; Sigfusson, B.; Gunnarsson, I.; Aradottir, E. S.; Alfredsson, H. A.; Gunnlaugsson, E.; Broecker, W. S. Monitoring Permanent CO2 Storage by in Situ Mineral Carbonation Using a Reactive Tracer Technique. *Energy Procedia* **2014**, *63*, 4180−4185.
(221) Bartels, M. F.; Miller, Q. R. S.; Cao, R.; Lahiri, N.; Holliman, J. E.; Stanfield, C. H.; Schaef, H. T. Parts-Per-Million Carbonate Mineral Quantification with Thermogravimetric Analysis−Mass Spectrometry. *Anal. Chem.* **2024**, *96* (11), 4385−4393.
(222) Wang, Y.; Chen, Y.; Wang, W.; Jiang, F.; Dou, W.; Su, M.; Bao, Z. Experimental Research System and Efficiency Evaluation Method of CO2 Sequestration in Basalt Mineralization. *Energy Fuels* **2024**, *38* (15), 14414−14421.
(223) Fawad, M.; Mondol, N. H. Monitoring Geological Storage of CO2 Using a New Rock Physics Model. *Sci. Rep.* **2022**, *12* (1), No. 297.